ELSEVIER

Neurobiology of Aging 34 (2013) 770–790

NEUROBIOLOGY OF AGING

www.elsevier.com/locate/neuaging

PP2A blockade inhibits autophagy and causes intraneuronal accumulation of ubiquitinated proteins

Amandine Magnaudeix[a], Cornelia M. Wilson[a,b], Guylène Page[c], Chantal Bauvy[d], Patrice Codogno[d], Philippe Lévêque[e], François Labrousse[f], Manuela Corre-Delage[f], Catherine Yardin[a,b], Faraj Terro[a,b,*]

[a] *Laboratoire d'Histologie, de Biologie Cellulaire et de Cytogénétique, Faculté de Médecine, Université de Limoges, Limoges, France*
[b] *Service d'Histologie et de Cytogénétique, Hôpital de la Mère et de l'Enfant, Limoges, France*
[c] *EA 3808 "Cibles moléculaires et Thérapeutique de la maladie d'Alzheimer"*
[d] *INSERM U984, Faculté de Pharmacie, Université Paris-Sud, Châtenay-Malabry, France*
[e] *CNRS, UMR 6172, XLIM - OSA Department, University of Limoges, Limoges, France*
[f] *Department of Pathology, Dupuytren University Hospital, Limoges, France*

Received 7 June 2011; received in revised form 30 May 2012; accepted 29 June 2012

Abstract

Using cultured cortical neurons, we show that the blockade of protein phosphatase 2A (PP2A), either pharmacologically by okadaic acid or by short hairpin RNA (shRNA)-mediated silencing of PP2A catalytic subunit, inhibited basal autophagy and autophagy induced in several experimental settings (including serum deprivation, endoplasmic reticulum stress, rapamycin, and proteasome inhibition) at early stages before autophagosome maturation. Conversely, PP2A upregulation by PP2A catalytic subunit overexpression stimulates neuronal autophagy. In addition, PP2A blockade resulted in the activation of the negative regulator of autophagy mammalian target of rapamycin complex 1 and 5' adenosine monophosphate (AMP)-activated protein kinase (AMPK) and led to intraneuronal accumulation of p62- and ubiquitin-positive protein inclusions, likely due to autophagy downregulation. These data are consistent with previous findings showing that specific invalidation of the autophagy process in the nervous system of mouse resulted in the accumulation of p62- and ubiquitin-positive protein inclusion bodies. Furthermore, we showed that PP2A inhibition alters the distribution of the microtubule-associated protein 1 light chain(LC) 3-I (MAP LC3-I), a key component of the autophagy molecular machinery. Whether MAP LC3-I distribution in the cell accounts for autophagy regulation remains to be determined. These data are important to human neurodegenerative diseases, especially Alzheimer's disease, because they provide links for the first time between the pathological features of Alzheimer's disease:PP2A downregulation, autophagy disruption, and protein aggregation.

Keywords: Autophagy; Neuron; PP2A; Protein aggregation; Alzheimer's disease

1. Introduction

Mammalian cells have 2 major and complementary catabolic pathways to get rid of abnormal proteins: the ubiquitin-proteasome system (UPS) and the autophagy/lysosomal pathway. Depending on the route of cargo delivery to the lysosomes, autophagy can be divided into 3 pathways: macroautophagy, microautophagy, and chaperone-mediated autophagy (CMA) (Mizushima et al., 2008; Pandey et al., 2007; Rideout et al., 2004; Rubinsztein, 2007). Macroautophagy—hereafter referred to as "autophagy"—is the main pathway for protein and organelle degradation in the lysosome. Autophagy exists in all eukaryotic cells at basal constitutive level and plays a crucial role in cell homeostasis

* Corresponding author at: Laboratoire d'Histologie, de Biologie Cellulaire et de Cytogénétique, Faculté de Médecine, 2 rue du Dr Raymond Marcland, 87025 Limoges CEDEX, France. Tel.: +33 5 55 43 58 93; fax: +33 5 55 43 58 93.
E-mail address: faraj.terro@unilim.fr (F. Terro).

0197-4580/$ – see front matter © 2013 Elsevier Inc. All rights reserved.
http://dx.doi.org/10.1016/j.neurobiolaging.2012.06.026

and protein quality control. Autophagy can also be induced and act as a defense response to stress conditions (adaptative autophagy) including metabolic stress like growth factor (Young et al., 2009), glucose or amino acid deprivation, UPS inhibition (Pandey et al., 2007; Rideout et al., 2004; Rubinsztein, 2007), and endoplasmic reticulum (ER) stress (Hetz et al., 2009; Lépine et al., 2011; Nijholt et al., 2011). During autophagy an isolating membrane forms, elongates, and surrounds the cellular material to be degraded, and the edges of this membrane fuse to form a double-membrane organelle, the autophagosome. Autophagosomes are then transported along the microtubules, toward the centrosome, where the autophagosome matures by fusing with vesicles of the lysosomal pathway (endosomes, lysosomes. . .) to acquire lysosomal enzymes (e.g., the proteases cathepsins) required for the degradation of the sequestered material (Kimura et al., 2008).

Basal autophagy is crucial, especially in postmitotic cells, like neurons, which cannot dilute their waste by cell division. Therefore, specific suppression of constitutive autophagy in the central nervous system of mice leads to neurodegeneration and intraneuronal accumulation of ubiquitinated protein inclusions in neurons (Hara et al., 2006; Komatsu et al., 2006). Interestingly, induction of autophagy in cell and animal models of neurodegenerative diseases by the mammalian target of rapamycin (mTOR) inhibitor, rapamycin has been shown to clear toxic proteins and aggregates regardless of the type of pathological protein (tau, superoxide dismutase 1, alpha-synuclein, huntingtin, rhodopsin. . .) (Berger et al., 2006; Midorikawa et al., 2010; Morimoto et al., 2007; Ravikumar et al., 2004; Rideout et al., 2004; Sarkar et al., 2009; Webb et al., 2003).

Autophagy is mainly regulated by the mTOR signaling pathway, especially the complex mTORC1 which negatively controls autophagy (Codogno and Meijer, 2005), although mTOR-independent autophagy has been documented (Sarkar et al., 2005, 2007, 2009, Shintani et al., 2010; Williams et al., 2008).

Beclin-1 positively regulates autophagy by promoting the activity of the class III PI3K Vps34, a kinase involved in the nucleation and expansion of an isolating membrane (Zeng et al., 2006). Interestingly, Beclin-1 expression was reported to be decreased in the brains of Alzheimer's disease (AD) patients and a partial deletion of the Beclin-1 gene in transgenic mice disrupted lysosomal function resulting in neurodegeneration and increased extracellular deposition of Abeta (Pickford et al., 2008).

5' Adenosine monophosphate (AMP)-activated protein kinase (AMPK) is an energy sensor that is activated by liver kinase B1 when cellular adenosine triphosphate (ATP) levels decrease (AMP:ATP ratio increases), for example under low glucose concentration (Fogarty and Hardie, 2010; Williams and Brenman, 2008). The axis liver kinase B1-AMPK negatively regulates mTOR and is further expected to induce autophagy.

p62/sequestosome-1 is implicated in the selective autophagy of certain protein aggregates, termed "aggrephagy" (Knaevelsrud and Simonsen, 2010). p62 binds to ubiquitinated proteins and self-polymerizes to form p62- and ubiquitin-positive protein inclusions. It also interacts, through its LC3-interacting region (LIR) domain with the microtubule-associated protein 1 light chain(LC) 3 (MAP1 LC3 or to simplify LC3) and thereby promotes the degradation of protein aggregates by autophagy. Therefore, p62 is itself degraded by autophagy (Bjørkøy et al., 2005), and inhibition of the autophagic flux or inhibition of lysosomal activity leads to the accumulation of p62 as well as LC3-II (Mizushima and Yoshimori, 2007; Ni et al., 2011).

Alterations in the endocytic/autophagic/lysosomal pathways were documented in AD brains (Cataldo et al., 1996; Nixon, 2006, 2007; Nixon et al., 2000, 2005). Concerning autophagy, a marked accumulation of immature autophagic vacuoles (AVs), especially autophagosomes, has been reported in dystrophic neurites (Nixon et al., 2005). The massive accumulation of immature AVs in dystrophic neurites led to the suggestion that the retrograde transport of autophagosomes and their maturation to autolysosomes may be altered, thereby interfering with neuroprotective function of autophagy (Nixon et al., 2005). This, however, does not exclude the possibility that an induction of autophagy may account for the accumulation of immature AVs. Data from cell and animal models of AD suggest that the net accumulation of immature AVs may constitute a source for Abeta generation because the autophagic vacuolar compartment was reported to be highly enriched in protein components of the machinery required for Abeta production (Yu et al., 2004) and Abeta can be generated, in a presenilin-1-dependent manner, by the induction of autophagy by rapamycin (Nixon, 2007; Yu et al., 2005).

Protein phosphatase 2A (PP2A) is a highly conserved heterotrimeric holoenzyme. In mammalian species, PP2A accounts for the majority of tau protein phosphatase activities in the brain (Xu et al., 2008). In AD brains, PP2A Messenger RNA (mRNA) and enzymatic activity were reported to be decreased (Gong et al., 1993; Vogelsberg-Ragaglia et al., 2001), whereas endogenous Inhibitor-1 of PP2A was increased (Chen et al., 2008; Tanimukai et al., 2005). PP2A downregulation is thought to contribute to tau hyperphosphorylation and aggregation, as well as Abeta production linked AD (Sontag et al., 2007). However, the role of PP2A in the autophagy process remains controversial. PP2A activity can be regulated by the association of its catalytic subunit (PP2Ac) with an unusual regulatory subunit α4 or Tap42 in yeast (Chen et al., 1998; Nanahoshi et al., 1998; Prickett and Brautigan, 2006). Depending upon cell type, the association PP2Ac-α4/Tap42 can or cannot be sensitive to rapamycin uncovering links between mTOR and PP2A signaling pathways. In yeast, inactivation of Tap42 induces autophagy in the presence or not of rapamycin and the inhibitory action of Tap42 on autophagy is

Table 1
Summary of the antibodies used

Source (clone)	Targeted protein	Catalogue reference	Company	Dilution	Incubation temperature
Rabbit	LC3	NB100-2220	Novus Biologicals	1/750 (IF)	RT
Rabbit	LC3	PM052	MBL	1/1000 (WB)	RT
Mouse	LC3	LC3; M152-3	MBL	1/200 (IF)	RT
Rabbit	p62	PM045	MBL	1/2000 (WB); 1/1000 (IF)	RT
Rabbit	PP2A-C	2038	Cell Signaling Technology	1/1000 (WB) Immuno-immobilization (10 μg/mL)	4 °C RT
Rabbit	p-PP2Ac (Y307)	115-S	Epitomics	1/1000 (WB)	4 °C
Rabbit	mTOR	2972	Cell Signaling Technology	1/1000 (WB)	4 °C
Rabbit	Phospho-mTOR (Ser 2448)	2971	Cell Signaling Technology	1/1000 (WB)	4 °C
Rabbit	P70S6K	9202	Cell Signaling Technology	1/1000 (WB)	4 °C
Mouse (1A5)	Phospho-P70S6K (Thr 389)	9206	Cell Signaling Technology	1/1000 (WB)	4 °C
Rabbit (23A3)	AMPK	2603	Cell Signaling Technology	1/1000 (WB)	4 °C
Rabbit (40H9)	Phospho-AMPK (Thr 172)	2535	Cell Signaling Technology	1/1000 (WB)	4 °C
Rabbit	ACC	3676	Cell Signaling Technology	1/1000 (WB)	4 °C
Rabbit (C83B10)	Phospho-ACC (Ser 79)	3661	Cell Signaling Technology	1/1000 (WB)	4 °C
Rabbit	Beclin-1	3738	Cell Signaling Technology	1/1000 (WB)	4 °C
Rabbit (R-20)	Cathepsin D	sc-6487	Santa-Cruz	1/1000 (WB)	RT
Rabbit	LAMP-2a	51-2200	Invitrogen	1/1000 (WB)	RT
Mouse (P4D1)	Ubiquitin	64301	BioLegend	1/1000 (WB); 1/200 (IF)	RT
Mouse (T46)	Tau (a phospho-independent epitope)	T9450	Sigma-Aldrich	1/2000 (WB); 1/1000 (IF)	RT
Mouse (PC1C6)	Nonphospho-tau (Tau-1)	MAB3420	Millipore	1/5000 (WB)	RT
Mouse (AT8)	Phospho-tau	AT-8	Pierce	1/1000 (WB)	RT
Mouse (12E8)	Phospho-tau	12E8	Seubert et al. (1995)	1/3000 (WB)	RT
Mouse (AC-40)	Actin	A0483	Sigma-Aldrich	1/5000 (WB)	RT
Mouse (5G8)	β-III-tubulin	G7121	Promega	1/5000 (WB) 1/1000 (IF)	RT
Rabbit	PP4 catalytic subunit (PPP4C)	ab16475	Abcam	Immuno-immobilization (10 μg/mL)	RT

Detailed information concerning the animal sources, company, dilution used in immunofluorescence (IF) or Western blot (WB) assays and incubation temperature with the indicated primary antibody are given. Tau phosphorylation was assessed using the following phospho-dependent anti-tau antibodies: Tau-1, 12E8 and AT-8. According to the residue numbering of the longest human tau isoform of 441 amino acids, Tau-1 recognizes tau only when serines (Ser) 195, 198, 199, and 202 are not phosphorylated, 12E8 detects tau phosphorylated at serine 262 and to a lesser extent at serine 356 (Seubert et al., 1995) and AT-8 recognizes tau when phosphorylated at serine 202 and threonine (Thr) 205. MBL (Woburn, MA, USA, distributed in France by Clinisciences Nanterre, France) , Novus biologicals (Littleton, CO, USA, distributed in France by Interchim, Montluçon, France), Cell signalling technology (Danvers, MA, USA, distributed in France by Ozyme, Saint-Quentin-en-Yvelines, France), Epitomics (Burlingame, CA, USA, distributed in France by Clinisciences, Nanterre, France), Pierce and Invitrogen (Thermo Fisher Scientific, Illkirch, France), Santa Cruz biotechnology (Heidelberg, Germany), Abcam (Paris, France), Millipore (Molsheim, France)

Key: ACC, Acetyl CoA carboxylase; AMPK, 5' adenosine monophosphate (AMP)-activated protein kinase; LAMP, ; LC, MAP LC3; mTOR, mammalian target of rapamycin; PP2A, protein phosphatase 2A; p-PP2Ac, phosphorylated catalytic subunit of PP2A; RT, room temperature.

mediated by mTOR-PP2A axis (Yorimitsu et al., 2009). Conversely, in mammalian cells, an association between PP2Ac and α4 downregulates PP2A activity toward specific substrates of the mTOR pathway (Nanahoshi et al., 1998) and the interaction between PP2Ac and α4 can be disrupted by rapamycin (Trockenbacher et al., 2001) which likely explains the activation of PP2A during rapamycin-induced autophagy (Park et al., 2008). In hepatocytes, inhibition of PP2A by okadaic acid (OKA) negatively regulates autophagy (Holen et al., 1993). Conversely, long-term exposure of cultured neurons to OKA and infusion of rat brains with OKA paradoxically activates mTOR (and mTOR substrate phosphorylation) and leads to the accumulation of autophagosomes (Yoon et al., 2008).

In AD, whether PP2A downregulation and autophagy impairment are linked remains to be determined. Given the interconnections between PP2A, mTOR, and AMPK pathways and the role of PP2A in the regulation of microtubule-associated protein (MAP) phosphorylation and microtubule dynamics, we have extensively analyzed the impact of the blockade of PP2A activity on autophagy in primary cultured neurons and its consequences on ubiquitinated protein accumulation.

2. Methods

2.1. Reagents and antibodies

Antibodies used in this study are listed in Table 1. MG132 (carbobenzoxy-Leu-Leu-leucinal), rapamycin, tunicamycin, leupeptin, pepstatin A, and okadaic acid (OKA) were purchased from Sigma-Aldrich Chemie (Saint-Quen-

tin Fallavier, France). Culture media and fetal calf serum were from Invitrogen (ThermoFisher Scientific, Illkirch, France). Unless otherwise indicated in the text, all other reagents were purchased from Sigma-Aldrich Chemie.

2.2. Primary neuronal cultures and treatments

All experimental protocols were approved by the local Ethics Committee.

Cortical cells were isolated from the brains of Wistar rat embryos (embryonic day 17.5) as previously described (Martin et al., 2009). The culture medium consisted of Neurobasal medium (Invitrogen) supplemented with B27 (1/50 dilution), glucose (18.0 mM), glutamine (2.0 mM) and 5% fetal calf serum. Cells resuspended in the culture medium were seeded into poly-L-lysine coated 35-mm Petri dishes, 6-well plates and 12-mm glass coverslips placed in 24-well plates. Cells were kept in an incubator at 37 °C under 5% CO_2 humidified atmosphere. Seven day-old in vitro cultures were used in the experiments.

2.3. Overexpression and lentivirus-mediated RNA interference of PP2Ac

For PP2Ac overexpression, SH-SY5Y cells were maintained in RPMI1640 medium supplemented with 10% fetal bovine serum, 5 mM glutamine, and grown at 37 °C with 5% CO_2. The cells in 6-well dishes were transiently transfected with PP2Ac cDNA (a generous gift of Dr. Judith Haendeler, University of Frankfurt) using JetPEI (Ozyme, France) for 18 hours before treatments.

To knockdown PP2Ac expression in rat primary cortical neurons, we used 2 commercially available pLKO.1-lentiviral shRNA vectors containing hairpin sequences targeting PP2CA (Open Biosystems, Thermo Fisher Scientific). The PP2Ac hairpin sequences were as follows with underlined sequencing corresponding to region of the *PP2ACA* gene targeted: CCG GCACACAAGTTTATGGTTTCTAC TCGAGTAGAAAC-CATAAACTTGTGTGTTTTT and CCGGGAGGGATATA-ACTGGTGCCA TCTCGAGATGGCACCAGTTATATCC-CTCTTTTT. In addition, we used the pLKO.1 lentiviral shRNA vector containing a hairpin sequence targeting dolichyl-diphosphooligosaccharide-protein glycosyltransferase, OST48 (Sigma) with the following sequence underlined corresponding to the region of the rat *OST48* gene targeted used as nonrelevant control: CCGGCCCTTTGACGGAGATGACATTCTCGAGAATGTC-ATCTCCGTCAAAGGGTTTTTG. The shRNA-containing lentiviral vector was cotransfected with pMDG-VSVG (vesicular stomatitis virus envelope protein) and p8.91 HIV-1 gag-pol expression vectors into HEK-293T cells to produce shRNA-carrying lentivirus particles. Culture supernatants were collected at 24, 48, 72, and 96 hours after transfection, filtered through a 0.45-μm filter (Millipore) and stored at −80 °C. Prior to infection, the lentivirus particles were concentrated by centrifugation at 38,000*g* in an SW28 rotor for 2 hours. The pellet was resuspended in 1/10 volume Neurobasal media. The viral titers were measured using HEK-293T and SH-SY5Y cell lines with a typical titer of 10^8 to 10^9 viral particles/mL. Rat primary cortical neurons were infected with the concentrated lentiviral stocks at 20–50 multiplicity of infection for 24 hours and the media was replaced with Neurobasal medium removed at the beginning of the infection. Cell lysates were harvested 48 hours postinfection. A pLKO.1 lentivirus containing no shRNA sequence was used as the negative control for the knockdown experiments.

2.4. Assessment of lysosomal activity and long-lived protein degradation

Primary cultured cortical cells were incubated with 25 nM OKA or with vehicle dimethyl sulfoxide (DMSO) for 6 hours. Then, they were washed twice in phosphate buffered saline and trypsinized at room temperature (RT) for 3 minutes. Trypsinized cells from 5 wells (1 sample as a total control) were pooled and resuspended in ice-cold 4 mL KHM buffer (110 mM KOAc, 2 mM MgOAc and 20 mM 4-(2-hydroxyethyl)-1-piperazineethanesulfonic acid [HEPES] at pH 7.2) and 100 μg/mL Soyabean trypsin inhibitor. Cells were pelleted by centrifugation and washed in 10% unbuffered electrolyte-free sucrose. All samples were then resuspended in 0.5 mL 10% unbuffered sucrose, warmed to 37 °C and electrodisrupted by a single high voltage pulse (2 kV/1.2 μF) (Seglen et al., 2009). The disruptate was cooled on ice and mixed with an equal volume (0.5 mL) of phosphate-buffered sucrose (100 mM sodium phosphate, 2 mM dithiothreitol, 2 mM ethylenediaminetetraacetic acid (EDTA) and 1.75% sucrose, pH 7.5). The diluted disruptate was layered on top of an ice cold density cushion of phosphate-buffered Metrizamide/sucrose (8% Metrizamide, 50 mM potassium phosphate, 1 mM dithiothreitol, 1 mM EDTA, 0.05% sucrose, pH 7.5) and centrifuged at 4 °C for 30 minutes at 3750 rpm. The cell pellets containing intracellular membranes enriched in lysosomes were resuspended in ice-cold buffered isotonic sucrose (0.25 M sucrose, 10 mM HEPES, 1 mM EDTA, pH 7.3). The enrichment of lysosomes in the pellets was verified by Western blot detection of the lysosomal membrane receptor. To measure acid phosphatase activity, aliquots of each lysosomal preparation were sonicated prior to the assay and incubated with 50 μL 4-nitrophenyl phosphate at 37 °C for up to 20 minutes in 9-mM citrate buffer, pH 4.8. Reactions were stopped by the addition of 200 μL of 0.5 M NaOH and absorbance at 405 nm was measured with Multiskan FC (Thermo Fisher Scientific). An aliquot of each sample was also assayed for total protein using the Bio-Rad DC protein assay. Enzyme activity was expressed as nmol per minute per mg of total protein.

Cathepsin D maturation, assessed by Western blot, was also used as indicator of the lysosomal activity.

Total protein degradation in SH-SY5Y cells was measured by pulse-chase assay according to a previously published detailed protocol (Bauvy et al., 2009). Briefly, intra-

cellular proteins were labeled by incubating SH-SY5Y cells for 18 hours at 37 °C with 0.2 μCi/ml L-[U-14 C] valine (specific activity 266 mCi/mmol) (Amersham Biosciences, Amersham Biosciences, Saclay, France) in RPMI1640 medium supplemented with 10% fetal bovine serum. Cells were rinsed with culture medium to eliminate nonincorporated radiolabeled valine and returned to the initial culture medium containing 10 mM unlabeled valine for 1 hour to allow the degradation of short-lived proteins. Cells were preincubated or not with 25 nM OKA for 1 hour. To assess the effect of OKA on basal macroautophagy, cells were incubated for 4 hours in fresh culture medium containing 10 mM cold valine in the presence or not of 10 mM of the inhibitor of macroautophagy 3-methyladenine (3-MA), 25 nM OKA or 3-MA and OKA combined. To test the effect of OKA on adaptative (induced) macroautophagy, macroautophagy was induced by cell incubation for 4 hours in Earle's balanced salt solution (EBSS) (Invitrogen, Thermo Fisher Scientific) in the presence or not of 25 nM OKA combined or not with 10 mM 3-MA. Culture media were taken and proteins in the medium were precipitated with cold 10% trichloracetic acid. Acid-soluble radioactivity in the supernatants (corresponding to degraded proteins) and pellets (nondegraded proteins) was measured in liquid scintillation counter. Cells were rinsed twice with cold 10% trichloracetic acid and precipitates were dissolved by incubation at 37 °C with 0.2 M NaOH for 2 hours and radioactivity was measured. Protein degradation was expressed as the percentage of the initial total radioactivity incorporated (corresponding to total protein labeled) in the cells converted to acid-soluble radioactivity (degraded proteins) in the culture medium. Protein degradation assay was performed in triplicate.

2.5. Cell fractionation assay

Primary cortical neurons in 35-mm diameter Petri dishes were rinsed once with ice-cold homogenization buffer (80 mM piperazine-N,N'-bis(ethanesulfonic acid) (PIPES) buffer pH 6.8, 1.0 mM $MgCl_2$, 2.0 mM EGTA, 30% glycerol, 10 mM benzamidine, 50 μg/mL leupeptin, 1 mM phenylmethanesulfonylfluoride (PMSF), 10 μg/mL aprotinin, 10 μg/mL antipain, and 0.2 mM sodium orthovanadate) and then harvested by scrapping in 150 μL of homogenization buffer containing 0.5% Triton X-100. Cell extracts were incubated for 30 minutes at 4 °C by end-over-end rotation. Samples were then centrifuged at 16,000*g* for 10 minutes at 4 °C. The resulting pellets were resuspended in 1X Laemmli buffer without dithiothreitol (DTT) (2% sodium dodecyl sulfate [SDS], 10% glycerol, 60 mM Tris pH 6.8). Supernatants were mixed (1:1) with 2× Laemmli buffer (4% SDS, 20% glycerol, 120 mM Tris 1 M, p 6.8). Protein concentrations were determined using Bio-Rad D_C Protein Assay kit and samples were heat-denatured (90 °C for 10 minutes) in the presence of 50 mM dithiothreitol and 0.01% bromophenol blue.

2.6. Immunoblotting assay

Cortical cells in 35 mm dishes were rinsed with phosphate buffered saline, and proteins were extracted by scraping the cells in 150 μL of 1× Laemmli sample buffer. Lysates were then sonicated and centrifuged at 18,000*g* for 15 minutes. The resulting supernatants were harvested, and protein concentrations were determined by Bio-Rad D_C Protein Assay. Samples were heat-denatured as described above. Depending on the primary antibody used in Western blot assay, 5–20 μg of total protein were separated by SDS-polyacrylamide gel electrophoresis (for a better separation of LC3-I and LC3-II, 15% polyacrylamide gels were used) then transferred to 0.45 μm polyvinylidene difluoride membranes (Millipore). Aspecific antigenic sites were saturated in 5% nonfat dry milk in Tris-buffered saline (TBS) containing 0.1% Tween 20 and membranes were probed with the appropriate antibodies (see Table 1). After incubation with the appropriate horseradish peroxidase-conjugated secondary antibodies (Bio-Rad, Marnes-la-Coquette, France) for 1 hour, proteins were detected with chemiluminescent substrate (Millipore) using G-Box (Syngene, UK). Densitometric analysis of Western blots was performed using GeneTools software 4.03 (Syngene, UK).

2.7. Immunofluorescence assay

Cells plated in 24-well plates containing glass coverslips were fixed with 4% paraformaldehyde in Sorensen's buffer (0.133 M Na_2HPO_4, 0.133 M $NaPO_4$ pH 7.4) for 20 minutes, rinsed with Sorensen's buffer and then permeabilized in 0.1% Triton X-100 in Sorensen's buffer. Cells were rinsed and incubated with primary antibodies overnight at 4 °C. Cells were rinsed again and aspecific antigenic sites were blocked by 5% normal goat serum for 1 hour. Cells were then probed with the appropriate Alexa-coupled secondary antibodies developed in goat (Invitrogen) during 1 hour at room temperature. Nuclear staining was performed with 4'-6-Diamidino-2-phenylindole (DAPI) (1 μg/mL) in Sorensen's buffer. Cells were mounted in mowiol medium and visualized using a fluorescence microscope (Eclipse-800, Nikon) with the appropriate fluorescence filters. Image acquisition was monitored with a charge-coupled device camera (Photonic Science, UK) using Visiolab (2000) software (Biocom, France). Pseudocolor images were mounted using Adobe Photoshop CS3 software.

2.8. Electronic microscopy

Primary cultured neurons were fixed by incubating the cells with 2% glutaraldehyde in 0.1 mM Sorensen's buffer, pH 7.4 for 30 minutes at RT. After 3 washes with Sorensen's buffer, cells were postfixed with 1% osmium tetroxide in Sorensen's buffer for 30 minutes (incubation in the dark at RT). Cells were then washed 3 times with Sorensen's buffer, dehydrated with 70% ethanol, 95% and 100% 3 times for 3 minutes. Almost all ethanol was removed and

cells were incubated with 100% resin (durcupan mixture) for 2 hours. Bean capsules filled with resin were placed upside down to the cells and resin was allowed to polymerize at 45 °C overnight and then at 60 °C for 2–3 hours. Sections of 70–100 nm were cut using a diamond knife and stained with uranyl acetate and lead citrate.

2.9. Autophagic cell count

LC3 is a mammalian homologue of yeast Atg8 and in addition to its originally described function as interacting- and stabilizing-protein of microtubules, LC3 plays an important role in autophagosome biogenesis (Kabeya et al., 2000; Kimura et al., 2008). During the early steps of autophagy, the C-terminal fragment of LC3 is cleaved by the serine protease Atg4 B/autophagin-1 to yield a cytosolic form, LC3-I. This cleavage exposes a glycine residue in the C-terminus allowing the modification of LC3-I by phosphatidylethanolamine through ubiquitin-like conjugation reactions (Ichimura et al., 2000; Tanida et al., 2004). Then the resulting lipidated form of LC3, LC3-II, associates with both inner and outer membranes of autophagosomes and the amount of LC3-II correlates with autophagosome formation (Kabeya et al., 2000).

To determine the percentage of autophagic cells, at least 200 cells in each experimental condition were examined. Bright LC3-positive vesicles with size of about 0.5–1.0 μm were counted as autophagic vacuoles (Lee et al., 2011) and cells with at least 2 distinct vacuoles were considered as autophagic cells (Kanzawa et al., 2005).

2.10. Statistical analysis

All data were expressed as mean ± SD and were analyzed for statistical significance by 1-way analysis of variance followed by the Student *t* test and *p* values < 0.05 were considered as significant.

3. Results

3.1. Exposure of cultured cortical neurons to OKA reduces the conversion of LC3-I into LC3-II by inhibiting autophagy upstream of the autophagosome maturation step

Opposing data were previously reported concerning the effect of PP2A blockade by OKA on neuronal autophagy. Short-term (3 hours) inhibition of PP2A by OKA at 15 nM has been reported to inhibit autophagy in hepatocytes (Holen et al., 1993), whereas long-term (24 hours) exposure of cultured cortical neurons to OKA at 12 nM resulted in the accumulation of autophagosomes and an increase in the level of the conversion of LC3-I (cytosolic) into the lipidated form of LC3, LC3-II (autophagosomal), and this despite the activation mTOR, the negative regulator of autophagy (Yoon et al., 2008). Using the same cell model of primary cultured neurons we failed to confirm these data. On the contrary, in our experiments, exposure of cultured cortical neurons to OKA at 12.5 and 25 nM for 6 hours in basal conditions (exposure was performed using the conditioning culture medium [CM] which is a nutriment-rich medium composed of Neurobasal medium supplemented with serum and B27 supplement, see Methods) resulted in a significant reduction in the level of conversion of LC3-I into LC3-II as evidenced by determining the ratio LC3-II/LC3-I (Fig. 1A and B). It is important to mention that OKA concentration and time exposure provide an optimal and efficient inhibition of PP2A (Martin et al., 2009), and despite important neuron morphology alterations (disruption of the neurite network and changes of the neuronal cell body morphology), neuronal death, as revealed by the detection of cleaved caspase-3 and measurement of cell viability by the Methylthiazol tetrazolium (MTT) assay, was not substantial ($< 10\%$) (see Supplementary Fig. 1A). This indicates that OKA-induced decrease in LC3-I to LC3-II conversion occurs before the accomplishment of neuronal death. However, longer (9 and 12 hours) exposure of cultured neurons to OKA (12.5 and 25 nM) resulted in a massive neuronal death, as revealed by Western blot detection of cleaved caspase-3 (Supplementary Fig. 1B) rendering it difficult to study autophagy. Even, in these neurotoxic conditions, analysis of LC3-I conversion into LC3-II by Western blot detection of LC3 showed that long exposure to OKA resulted in a decrease in LC3-II (see Supplementary Fig. 1B). Furthermore, it is interesting to note that OKA-induced decrease in LC3-II was constantly parallel to a reproducible, while statistically nonsignificant, slight increase in LC3-I (LC3-I/actin) ($p = 0.063$ as compared with nontreated cultures) (see Fig. 1A for LC3 Western blot, quantification of LC3-I is not shown). Serum deprivation can be used as an inducer of autophagy in primary cultured neurons (Young et al., 2009). Exposure of cultured neurons to OKA under serum deprivation conditions (the conditioning medium replaced by serum-free MEM without glucose, to simplify these conditions were designated throughout the text and in figures as “MEM”) also reduced the rate LC3-II/LC3-I, indicating that inhibition of PP2A also impairs adaptative autophagy (Fig. 1A).

Several and nonmutually exclusive mechanisms might contribute to the OKA-induced “apparent” decrease in the conversion of LC3-I into LC3-II: first, a net and actual decrease in this conversion due to the inhibition of autophagy, and thus through alteration of signaling pathways (e.g., mTOR pathway) upstream of the core machinery of autophagosome formation, and secondly, an acceleration of the autophagic flux by promoting autophagosome-lysosome fusion and/or by the stimulation of LC3-II (of the inner autophagosomal membrane) degradation in autolysosomes. p62 is itself a substrate of autophagy (Bjørkøy et al., 2005) and inhibition of the autophagic flux yields to a marked accumulation of autophagic vacuoles and consequently p62 as well as LC3-II increase (Mizushima and Yoshimori, 2007; Ni et al., 2011).

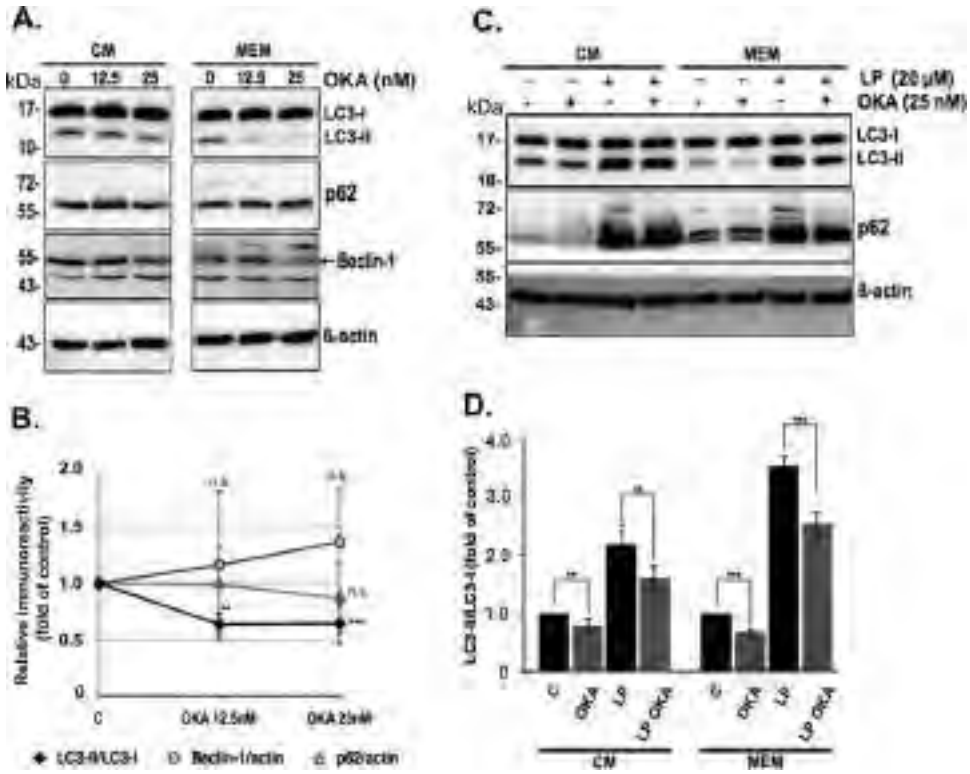

Fig. 1. Inhibition of autophagy in cultured neurons by okadaic acid (OKA). (A) Detection of LC3 forms (LC3-I and LC3-II) p62 and Beclin-1 by Western blot. Cultured neurons were incubated in the presence or absence of OKA at 12.5 nM and 25 nM in basal conditions (conditioned medium; CM) or under glucose and serum deprivation conditions (Minimum Essential Medium without glucose; MEM) for 6 hours and cell extracts were assayed by Western blot for LC3. β-actin was used as a loading control. (B) Semiquantitative analysis of LC3, p62 and Beclin-1 (only the band of about 55 kDa) immunoblots and calculation of the ratio LC3-II/LC3-I used to measure the conversion of LC3-I into LC3-II. (C and D) Analysis of the autophagic flux. Primary cultured neurons in conditioned medium (basal conditions) were pretreated with 20 μM leupeptin (L) and 20 μM pepstatin (P) or with vehicle DMSO and at 18 hours of treatment, OKA was then added to the medium (CM or MEM) for a further 6 hours. Autophagic flux was analyzed by immunoblot detection and semiquantitative analysis of LC3 and p62. Results are presented as means (expressed as fold of control) $\pm$ SD. All data are representative of at least 3 independent experiments and were analyzed for statistical significance with Student t test. * $p < 0.05$; ** $p < 0.01$; *** $p < 0.001$. Abbreviation: n.s., nonsignificant.

To test the possibility that OKA-induced decrease in LC3-II might result from an induction of autophagy and/or an acceleration of the autophagic flux, the autophagic flux was blocked by the inhibition of the lysosomal proteases cathepsins using leupeptin and pepstatin combined (Boland et al., 2008). For this purpose, primary cultured neurons in CM were pretreated with 20 μM leupeptin and 20 μM pepstatin or with vehicle DMSO and then additionally treated for 6 hours with or without 25 nM OKA. Similar experiments were performed using MEM without glucose (serum and glucose deprivation) instead of CM. Blockade of the autophagic flux by leupeptin and pepstatin resulted in a net increase of LC3-II (as well as the rate LC3-II/LC3-I) and p62 (Fig. 1C and D). In the absence of autophagic flux blockade, both in basal and serum deprivation conditions, OKA did not significantly alter p62 or that of Beclin-1 (see Fig. 1A for Western blots and Fig. 1B for semiquantitative analysis). These data exclude the possibility that cell exposure to OKA decreased LC3-II through acceleration of the autophagic flux and the stimulation of its degradation in the autolysosomes. If OKA induces autophagy and/or stimulates the autophagic flux, then it must yield an increase in LC3-II and p62 when the autophagic flux is blocked. Data presented in Fig. 1C and D show that, on the contrary, OKA-induced decrease of LC3-II/LC3-I is maintained, in basal (CM) as well as under serum and glucose deprivation, even when the autophagic flux was inhibited. For example, in basal conditions the ratio LC3-II/LC3-I was 2.2 $\pm$ 0.4 in cultures treated with leupeptin and pepstatin in the absence of OKA and 1.6 $\pm$ 0.2 in the presence of OKA.

Consistent with these Western blot data, the inhibitory action of OKA on autophagy was then confirmed by determining the percentage of autophagic cells (cells containing at least 2 autophagic vacuoles corresponding to LC3-positive vesicles with a size of about 0.5 μM or greater). The amount of LC3-II generally correlates with the number of autophagosomes in the cell and LC3-II is widely used as marker of autophagosomes (Kabeya et al., 2000; Kuma et al., 2007). In our model of cultured neurons, we confirmed previous findings showing that very few autophagic vacuoles are detected in basal conditions (Fig. 2A), likely due to a high efficiency of autophagic flux in neurons (Boland et

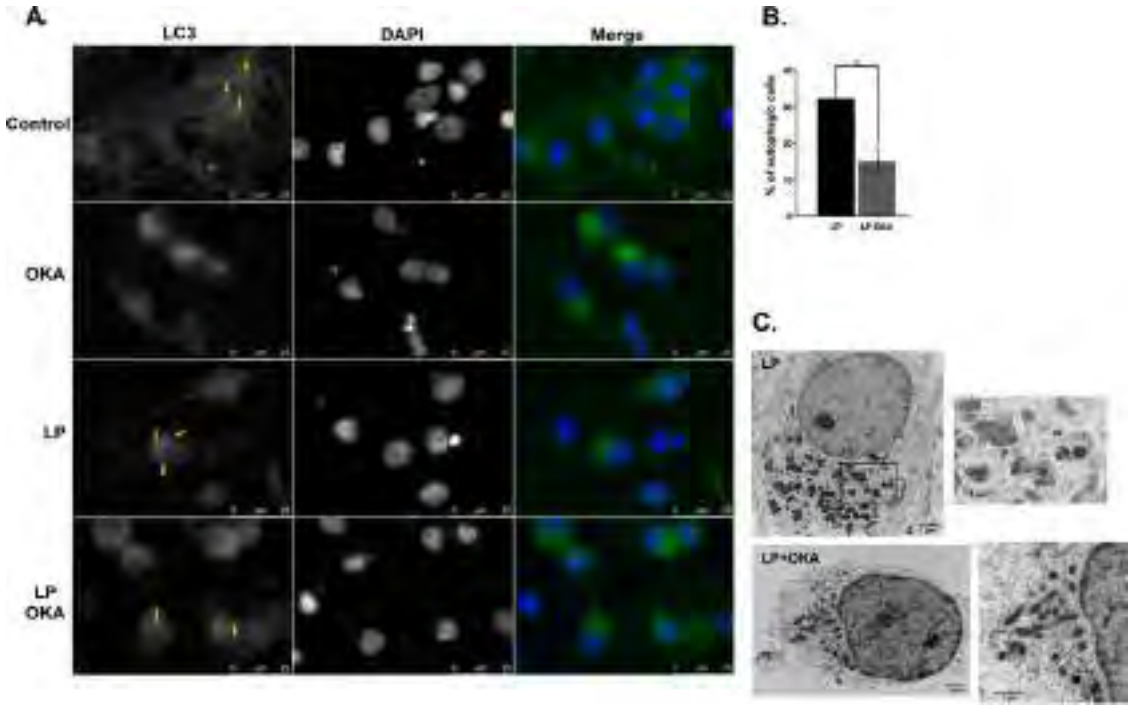

Fig. 2. In situ assessment of autophagy under conditions of protein phosphatase 2A (PP2A) blockade by okadaic acid (OKA). Autophagic vacuoles (AVs) were detected by LC3 immunofluorescence (A) and assessed by electronic microscopy (EM) morphometric analysis (C). (A) Detection of autophagic vacuoles by immunofluorescence detection of LC3 (green) in cells treated or not by OKA in the presence or absence of autophagic flux inhibitors, leupeptin and pepstatin (LP) at 20 μM. Cells were counterstained by the nuclear dye DAPI (blue). (B) Autophagic cell count. Cells containing more than 2 distinct autophagic vacuoles (LC3-positive bright punctuates with a ranging size of 0.5–1.5 μm; arrows). At least 20 microscope fields per 1 coverslip (about 200 cells) were examined and the percentage of autophagic cells (cells with at least 2 autophagic vacuoles) was determined. (C) EM morphometric analysis of autophagic vacuoles in conditions of autophagic flux blockade combined with (LP + OKA) or without (LP) OKA treatment. The blockade of autophagic flux by LP resulted in the accumulation of numerous AVs and treatment with OKA combined with inhibition of autophagic flux dramatically reduced the number of AVs. Results are expressed as mean ± SD. Data are representative of at least 3 independent experiments and were analyzed for statistical significance with Student *t* test. ** $p < 0.01$.

al., 2008). In order to facilitate the detection and counting of autophagic vacuoles, LC3 immunofluorescence was performed in condition of autophagic flux blockade by leupeptin and pepstatin. To confirm that OKA did inhibit autophagy, we determined the percentage of autophagic cells; a cell with at least 2 distinct AVs was considered as autophagic (Kanzawa et al., 2005). Cell exposure to 25 nM OKA in the presence of leupeptin and pepstatin (LP) significantly decreased the percentage of autophagic cells from 32.0% ± 3.8 (LP alone) to 14.8% ± 3.4 (LP + OKA) (Fig. 2B). Interestingly, and in accordance with Western blot data, OKA-treated cells exhibited an increased LC3 staining in the cytosol (background staining likely corresponding to LC3-I) and a concomitant decrease in the number of LC3-positive vesicles (Fig. 2A). A sharp decrease in the number of AVs was seen in individual cells exposed to OKA in the presence of LP (in Fig. 2A compare cells in control panel to cells in LP +OKA panel). Morphometric analysis by electronic microscopy (EM) cell imaging clearly confirmed these observations. Inhibition of cathepsins by leupeptin and pepstatin led to the accumulation of vesicles with dense and compacted amorphous contents (Fig. 2C, LP panel). These vesicles were previously demonstrated, for the majority, to be single membrane-limited and appear to be autolysosomes (Boland et al., 2008). Exposure to OKA dramatically decreased the number of autophagic vacuoles in cells cotreated by cathepsin inhibitors (Fig. 2C, LP + OKA panel). These data gathered indicate that OKA failed to stimulate the autophagic flux but rather inhibits autophagy at steps before the autophagosome maturation process. The fact that exposure of serum-deprived cells to OKA strongly reduced the ratio LC3-II/LC3-I and that the magnitude of this decrease is more important than that observed in basal conditions indicates that OKA not only inhibits constitutive basal neuronal autophagy but also autophagy induced by a metabolic stress.

3.2. Downregulation of PP2A by shRNA silencing of PP2A catalytic subunit inhibits autophagy

OKA is widely used as a potent, but relatively specific, inhibitor of PP2A because it also inhibits, while to a lesser extent (compared with PP2A), other protein phosphatases especially PP4 (Fujiki and Suganuma, 1993). In normal human brains, PP2A predominantly contributes to phosphatase activities (Liu et al., 2005). Due to the major contribu-

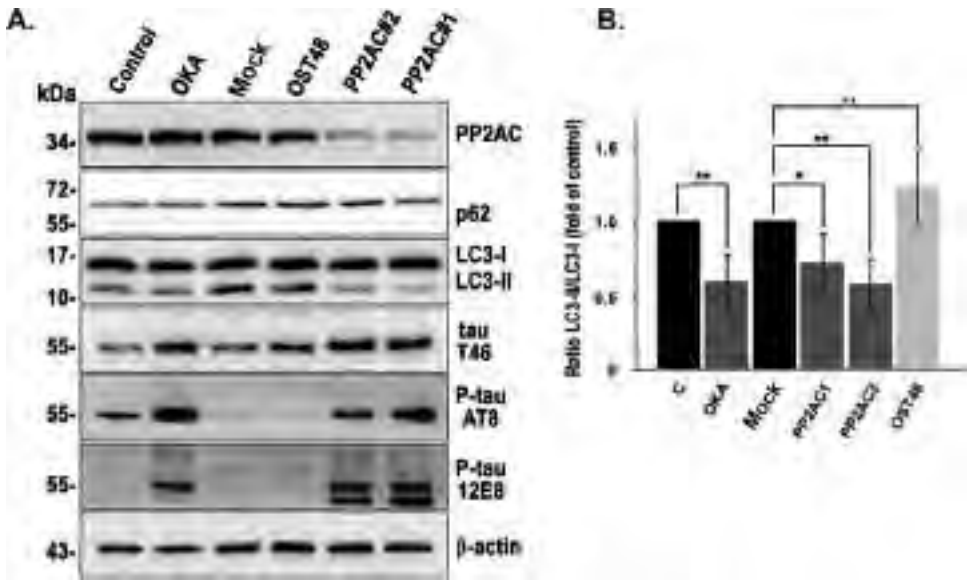

Fig. 3. Protein phosphatase 2A (PP2A) downregulation by shRNA-mediated silencing of the PP2A catalytic subunit and inhibition of autophagy. ShRNA-mediated PP2Ac knockdown was performed in cultured neurons using 2 sets of lentiviral constructs (shRNA PP2AC#1 and shRNA PP2AC#2). Silencing of the endoplasmic reticulum (ER) oligosaccharyltransferase (OST) complex protein, OST48 was used as an irrelevant control. To confirm the efficacy of PP2Ac silencing, cell extracts were subjected to immunoblot analysis for PP2Ac. Downregulation of PP2A enzymatic activity was tested by Western blot analysis of tau phosphorylation, a common neuronal substrate of PP2A, with the indicated anti-tau antibodies (see also Table 1). Autophagy was assessed by LC3 and p62 Western blot and by quantification of autophagic cells. (A) Immunoblot detection of PP2Ac, LC3, p62, phosphorylated and global tau, and β-actin used as a loading control. (B) Semiquantitative analysis of LC3 isoforms and determination of LC3-II/LC3-I ratio. Results are presented as mean (expressed as fold of control) $\pm$ SD. Data are representative of at least 3 independent experiments and were analyzed for statistical significance with Student t test. * $p < 0.05$; ** $p < 0.01$. Abbreviation: n.s., nonsignificant.

tion of PP2A to cellular phosphatase activity, it is expected that inhibition of cellular phosphatases by OKA in neurons is most likely due to the inhibition of PP2A. To determine whether OKA preferentially acts on PP2A, we measured the enzymatic activities of PP2A and that of a nonrelevant phosphatase PP4 in cell lysates isolated from cultured neurons exposed to OKA (25 nM, 6 hours) (see Supplementary data). As expected, PP2A activity was potently inhibited by OKA (Supplementary Fig. 1C). On the contrary, the same treatment with OKA did not significantly inhibit the activity of PP4A (Supplementary Fig. 1C). These results confirm the high specificity of OKA toward PP2A in rat primary cultured cortical neurons. To confirm that the action of OKA on autophagy is readily linked to PP2A blockade, PP2A activity was invalidated by shRNA knockdown of PP2Ac using lentiviral transfection. Knockdown of oligosaccharyltransferase (OST)48 was used as a nonrelevant control. PP2Ac depletion was analyzed at the protein level by Western blot using an anti-PP2Ac antibody and the downregulation of PP2A enzymatic activity was determined by Western blot analysis of phosphorylated tau, a common PP2A substrate, using the phosphodependent anti-tau antibodies AT8 and 12E8 (see Table 1). Compared with control, mock, or OST48 knockdown, silencing of PP2Ac using 2 different lentiviral preparations (shRNAPP2AC#1; shRNAPP2AC#2), as well exposure to OKA at 25 nM potently increased tau phosphorylation at both AT-8 and 12E8 sites (Fig. 3A). Analysis of autophagy indicates that as, observed with OKA, LC3-II/LC3-I ratio was significantly reduced after PP2Ac knockdown (1.0 vs. 0.7 $\pm$ 0.2 and 0.6 $\pm$ 0.2 respectively for each shRNA; $p <$ 0.05 and $p < 0.01$), whereas p62 levels were not significantly affected. Invalidation of PP2Ac-like exposure to OKA decreased the percentage of autophagic cells (Fig. 4A and B). Some AVs are found in the control and OST48-depleted neurons (Fig. 4A, compare control and OST48 panels) whereas in PP2A-depleted cells AVs are very rare (Fig. 4A, compare control and shRNA PP2Ac panel). These data indicate that specific depletion of PP2A negatively regulates basal neuronal autophagy.

3.3. PP2A activation by transient overexpression of PP2Ac induces autophagy

We then addressed the question of whether activation of PP2A positively regulates neuronal autophagy. For this aim, PP2Ac was overexpressed in SH-SY5Y cells and basal autophagy was analyzed in the presence or not of lysosomal inhibitors leupeptin and pepstatin (Fig. 5).

Western blot detection of PP2Ac showed that transfection of SH-SY5Y cells with PP2Ac cDNA resulted in an increase in PP2Ac protein levels (Fig. 5A). This increase in PP2Ac was associated with a decreased level of the inactive PP2Ac form (PP2Ac phosphorylated at residue Y307) and

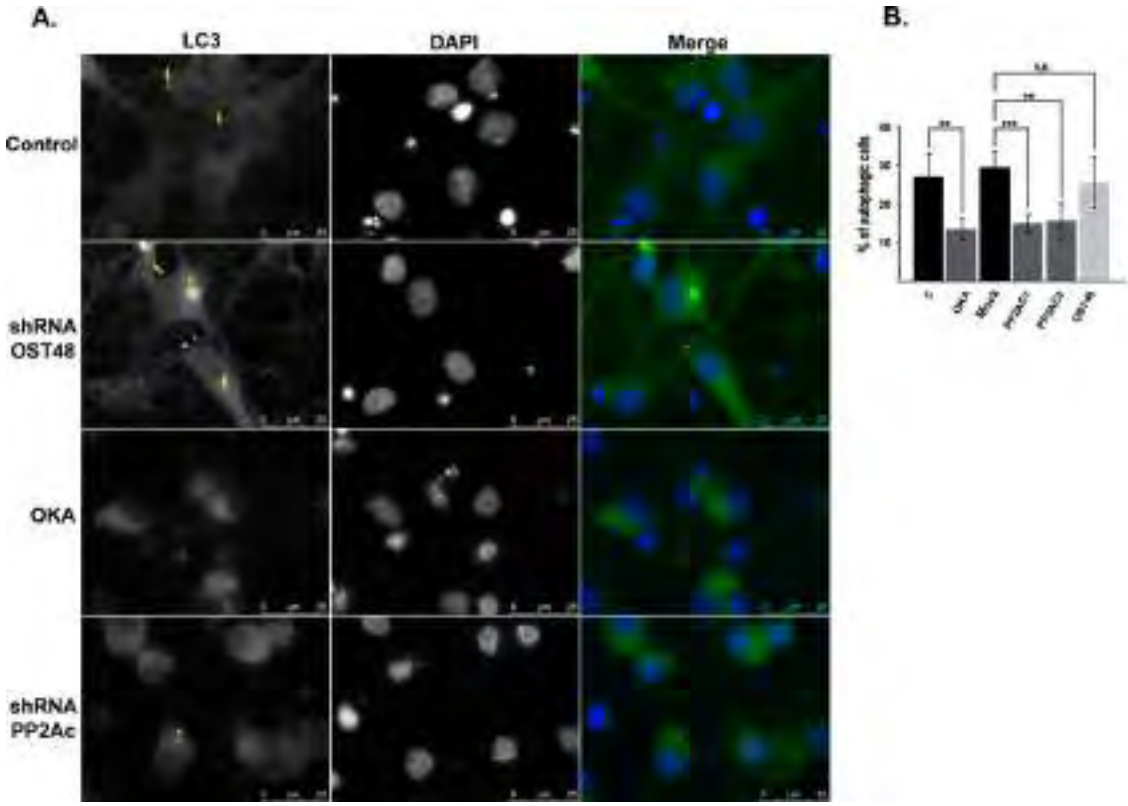

Fig. 4. In situ assessment of autophagy under conditions of protein phosphatase 2A (PP2A) blockade by okadaic acid (OKA). (A) Detection of autophagic vacuoles by immunofluorescence staining of LC3 (green). Cells were counterstained by the nuclear dye DAPI (blue). (B) Quantification of autophagic cells. Data are representative of at least 3 independent experiments and were analyzed for statistical significance with Student *t* test. ** $p < 0.01$; *** $p < 0.001$. Abbreviation: n.s., nonsignificant.

indirectly indicates that PP2A activity was upregulated (Fig. 5A). Activation of PP2A resulted in the increase of the conversion of LC3-I into LC3-II and blockade of the autophagic flux by LP accentuated this increase (Fig. 5A and B). PP2Ac overexpression did not significantly alter the levels of p62 and Beclin-1. Immunofluorescence detection of LC3 showed that, both in the absence or the presence of the autophagic flux inhibitors LP, PP2Ac overexpression increased the number of AVs (LC3-positive vesicles) whereas treatment with OKA appears to decrease this number. Similarly to what was observed in primary cultured neurons, exposure to OKA increased cytosolic LC3 (LC3-I). These data provide direct evidence that PP2A activation positively regulates basal autophagy independently of the positive autophagy regulator Beclin-1.

3.4. Inhibition of PP2A by OKA reduced long-lived protein degradation rate without directly altering the enzymatic lysosomal activities

To assess the lysosomal activity, the lysosomal acid phosphatase activity was measured in lysosome-enriched cell fractions. The level of the lysosomal membrane-associated protein 2a (LAMP-2a) was used as an indicator of lysosome enrichment in the cellular fractionation assay. LAMP-2a was mainly found in the pellet confirming that this fraction is enriched in lysosomes whereas the supernatant was enriched in βIII-tubulin, a neuronal cytoskeleton protein (Fig. 6A). Exposure of cultured neurons to OKA failed to significantly alter lysosomal acid phosphatase activity (Fig. 6B) or to affect cathepsin D maturation (Fig. 6C and D), another indicator of lysosome activity. These data indicate that inhibition of PP2A by OKA did not impair (directly) lysosomal function.

Assay for long-lived protein degradation in SH-SY5Y cells showed that OKA reduced protein degradation rate in basal conditions as well as in conditions where macroautophagy was induced by starvation during cell incubation in EBSS (Fig. 6E). Basal (control) protein degradation rate per hour was about 1.24% ± 0.09, cell exposure to OKA reduced basal protein degradation to 1.10% ± 0.13 which represents a decrease by 11.3%. This decrease was comparable with that obtained under cell incubation with 3-MA (15%), where the rate of protein degradation per hour was about 1.05% ± 0.17. An additive inhibitory effect on protein degradation rate was obtained under cell treatments with 3-MA and OKA combined; in these conditions, the rate of protein degradation was about 1.005 ± 0.03% which reflects a decrease by 18.9% of the basal rate. Exposure to

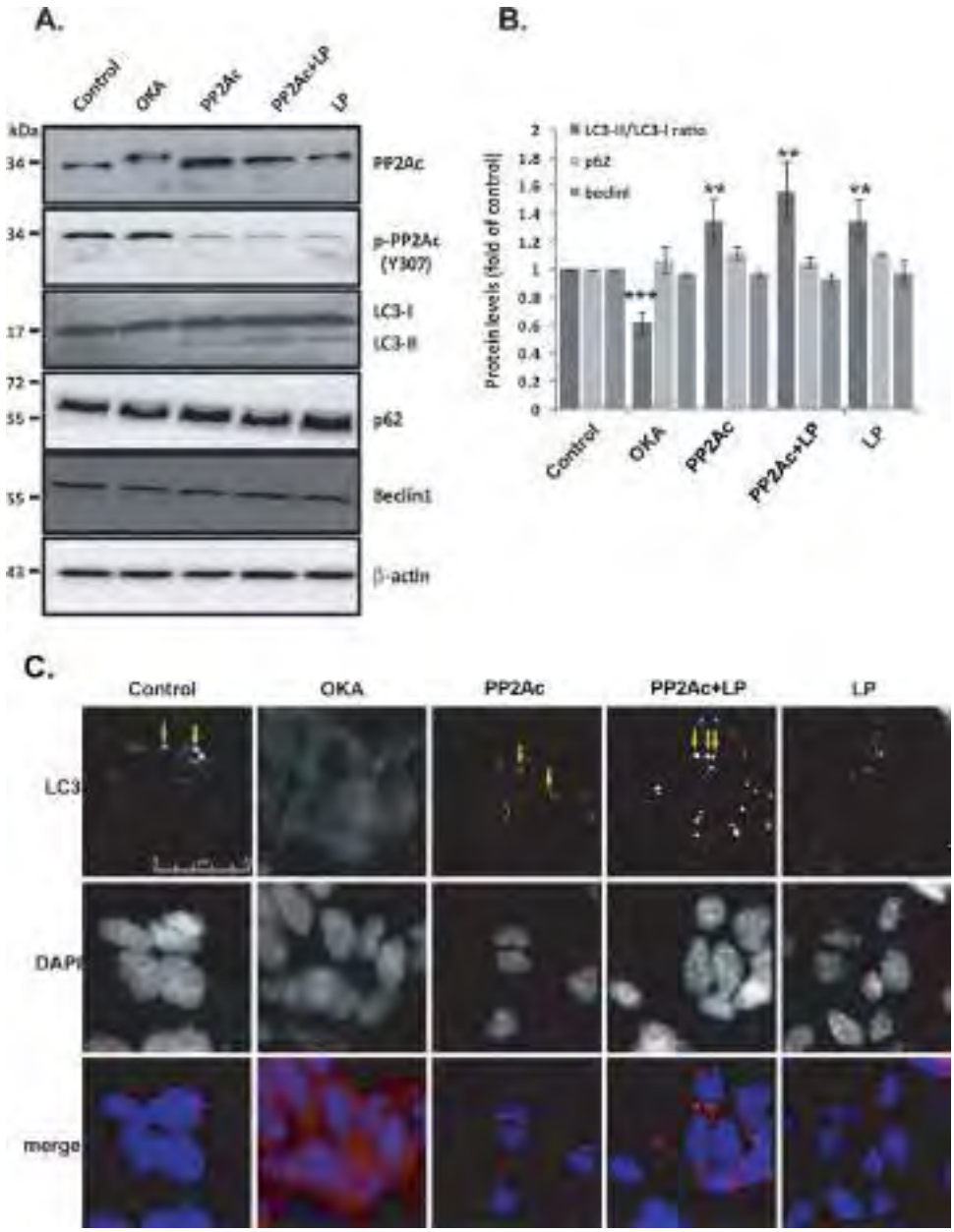

Fig. 5. Activation of protein phosphatase 2A (PP2A) by the overexpression PP2A catalytic subunit (PP2Ac) upregulates autophagy. PP2Ac was transiently overexpressed in SH-SY5Y cells (PP2Ac) and autophagy was assessed in the presence or absence of inhibitors of the autophagic flux, leupeptin and pepstatin (LP). Autophagy was also assessed in cells exposed to okadaic acid (OKA). (A) Western blot detection of native PP2Ac and phosphorylated PP2Ac at Y307 (p-PP2Ac), LC3, p62, Beclin-1, and β-actin. (B) Semiquantitative analysis of Beclin-1, p62, and LC3 (to determine the ratio LC3-II/LC3-I). (C) Detection of autophagic vacuoles (AVs) by LC3 immunofluorescence (red). Cells were counterstained by the nuclear dye DAPI (blue). Note that the activation of PP2A increased the number of AVs (arrows) whereas OKA increased LC3 staining in the cytoplasm and decreased the number of AVs. Data are representative of at least 3 independent experiments and were analyzed for statistical significance with Student *t* test. ** $p < 0.01$; *** $p < 0.001$ as compared with controls.

OKA also led to a marked downregulation of protein degradation observed under incubation of the cell in EBSS. The rate of protein degradation was 1.40 ± 0.10% in EBSS conditions. This value was reduced to 0.88 ± 0.03% (reduction by 41.9%), 0.97 ± 0.12% (reduction by 31%) and 0.92 ± 0.21% (reduction by 34.3%) respectively under cell exposure to 3-MA, OKA, and 3-MA + OKA respectively. In general, whereas macroautophagy is activated during the first hours of starvation (4–6 hours), CMA progressively increases after that time to reach a plateau of maximal activity at 20 hours of starvation in fibroblasts (Kaushik et al., 2008). This indicates that in our experimental conditions of autophagy induction by cell incubation in EBSS during 4 hours, macroautophagy and not CMA is activated. These data gathered indicate that inhibition of PP2A by OKA did downregulate the macroautophagy component of autophagy

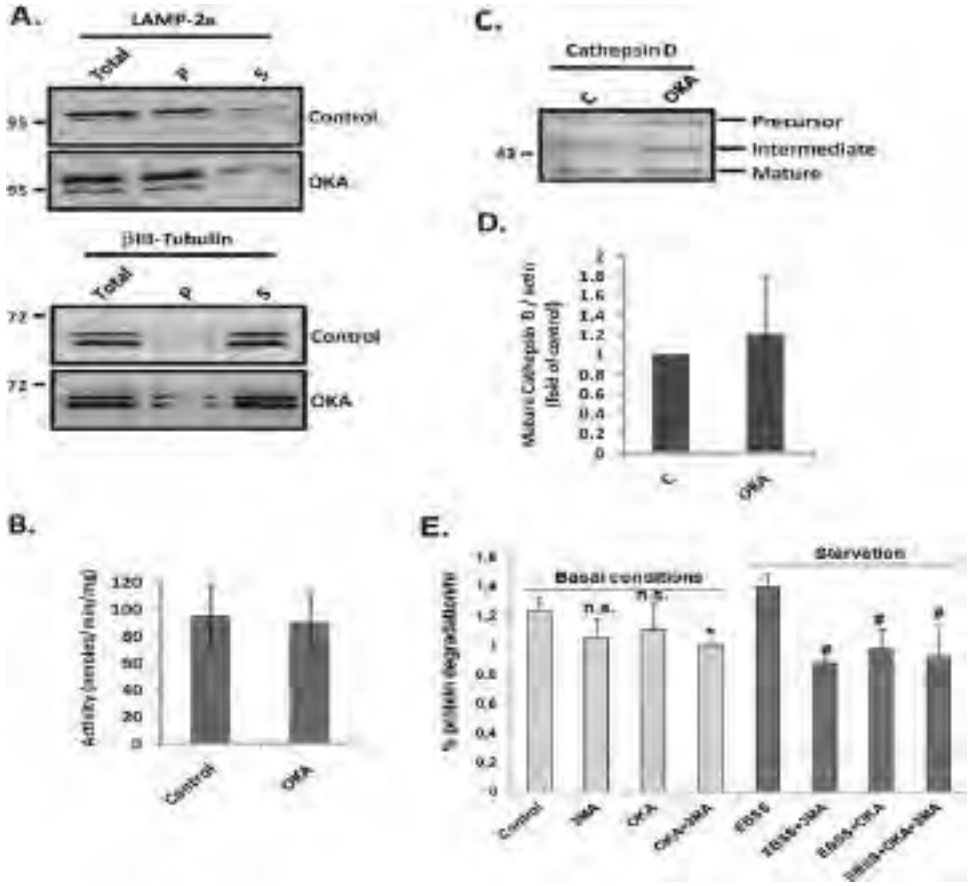

Fig. 6. Effects of protein phosphatase 2A (PP2A) inhibition by okadaic acid (OKA) on lysosome activity. Primary cultured neurons were exposed or not to OKA at 25 nM for 6 hours. Cells were then subjected to a cell fractionation assay and acid phosphatase activity was measured in lysosome-enriched fractions. Cathepsin processing from the precursor to the mature form was used as another marker of lysosome activity. (A) Western blot detection of LAMP-2a and βIII-tubulin. LAMP-2a was mainly found in the pellet while βIII-tubulin was found in the supernatant. (B) Measurement of acid phosphatase activity in the pellet, the lysosome-enriched fraction. (C and D) Analysis of cathepsin D activation by Western blot detection in total cell lysates (C) and semiquantitative analysis of cathepsin D (D). (E) Analysis of effect of the inhibition of PP2A on long-lived protein degradation. Intracellular protein degradation rate in SH-SY5Y was determined by pulse-chase experiments using L-[U-14 C] valine. The effect of OKA (25 nM, 4 hours) on protein degradation was tested in basal conditions (treatment was performed in complete culture medium) and in starvation conditions by incubating the cells in Earle's balanced salt solution (EBSS) during 4 hours. * $p < 0.05$ as compared with control; # $p < 0.05$ as compared with EBSS. Abbreviation: n.s., nonsignificant.

and this by acting at early steps of autophagy before the protein degradation process itself. Our data concerning the inhibitory action of OKA on autophagy are consistent with those obtained by Holen et al. (1993) who demonstrated that OKA inhibits autophagy in isolated rat hepatocytes.

3.5. Okadaic acid inhibits autophagy induced by various cell stresses

Autophagy can be induced by a number of cell stresses. Some authors discriminate constitutive autophagy from stress-induced autophagy (Komatsu and Ichimura, 2010; Komatsu et al., 2007a). We have demonstrated that OKA inhibits basal constitutive autophagy and autophagy induced by a metabolic stress resulting from serum and glucose deprivation, we sought to determine whether or not the inhibitory action of OKA on autophagy occurs regardless of the nature of the autophagy trigger, meaning that OKA (through the inhibition of PP2A) likely affects a common pathway which controls the core machinery of autophagy. To this aim, OKA was tested in primary cultured neurons challenged with several common inducers of autophagy including rapamycin (an inhibitor of mTOR), tunicamycin (inhibitor of N-glycosylation and an inducer of ER stress), MG132 (a UPS inhibitor) (Ding et al., 2007; Korolchuk et al., 2009; Nijholt et al., 2011; Ogata et al., 2006; Rideout et al., 2004; Rubinsztein, 2007; Yorimitsu et al., 2006). Rapamycin induces autophagy by inhibiting mTOR and thus mimicking a metabolic stress. In neurons, rapamycin increases the autophagic flux (Rubinsztein and Nixon, 2010). Cultured neurons were treated with 250 nM rapamycin for 18 hours and then additionally treated for 6 hours with 25 nM OKA. Rapamycin alone significantly increases the LC3-II/LC3-I ratio (1.0 vs. 2.2 ± 0.6; $p < 0.001$) and this increase was reversed by OKA (2.2 ± 0.6 vs. 1.2 ± 0.4; $p < 0.01$) (Fig. 7A and B). Induction of ER stress by exposure for 6 hours to 0.5 μg/mL tunicamycin resulted in

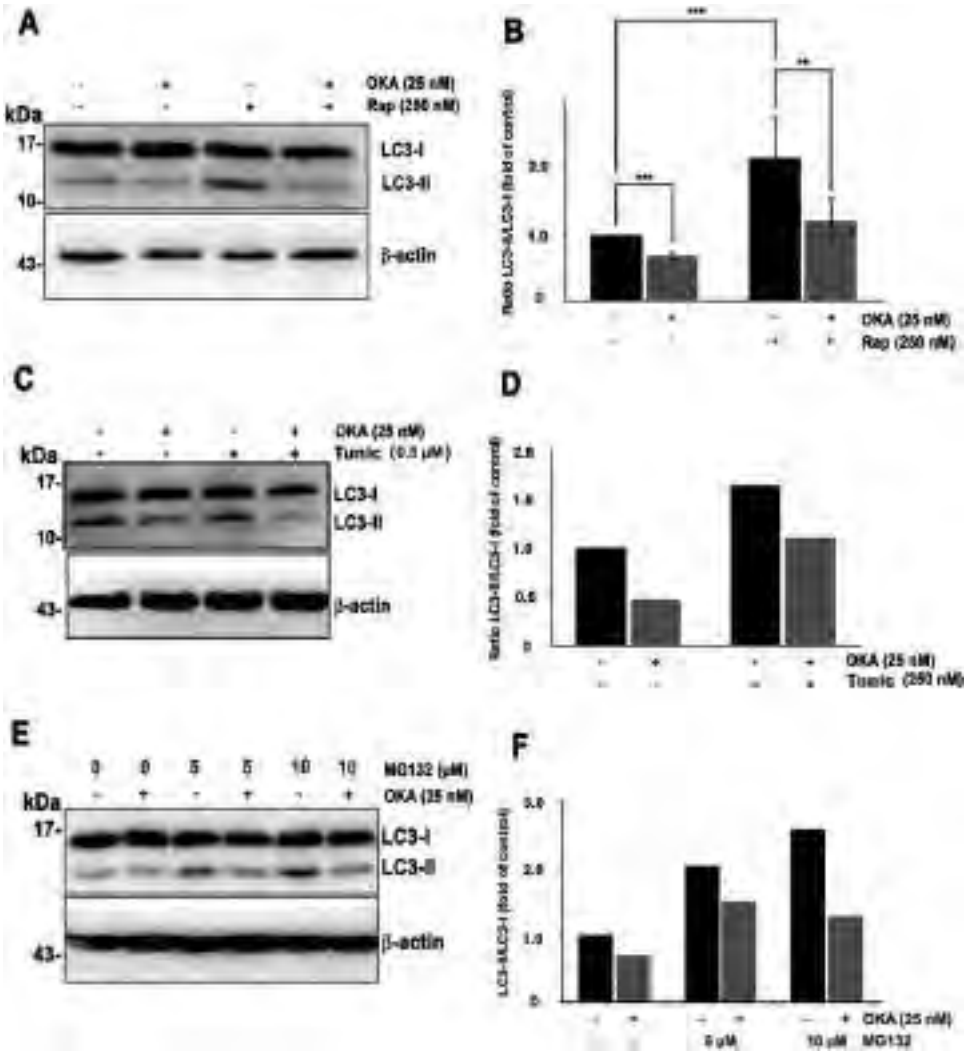

Fig. 7. Inhibition by okadaic acid (OKA) of autophagy induced by various stresses in cultured neurons. Cultured neurons were exposed to several known pharmacological inducers of autophagy including the inhibitor of mammalian target of rapamycin (mTOR) rapamycin (Rap) (250 nM), the endoplasmic reticulum (ER) stress inducer tunicamycin (Tunic) (0.5 μg/mL) and the proteasome inhibitor MG132 (5 and 10 μM), in the presence or absence of OKA. Treatment with rapamycin was performed for 18 hours and then OKA was added for a further 6-hour treatment (total 24 hours) whereas, exposure to Tunicamycin (Tunic) or MG132 was performed in the presence of OKA for 6 hours. Autophagy was then analyzed by Western blot detection of LC3 isoforms (LC3-I and LC3-II). (A, C, and E) Immunoblot detection of LC3 respectively in cultures exposed to rapamycin, TM, and MG132 in the presence or absence of OKA. β-actin was used as a loading control. (B, D, and F) Semiquantitative analysis of LC3 isoforms and calculation of the ratio LC3-II/LC3-I of cultures exposed to rapamycin, TM, and MG132 respectively in the presence or absence of OKA. Data were analyzed for statistical significance with Student *t* test. ** $p < 0.01$; *** $p < 0.001$. Abbreviation: n.s., nonsignificant.

an increase of the LC3-II/LC3-I ratio (Fig. 7C and D), which was reversed by the concomitant treatment with 25 nM OKA. Consistent with previous findings (Pandey et al., 2007; Rideout et al., 2004), in our experiments, inhibition of UPS by MG132 (5 and 10 μM for 6 hours) clearly increased LC3-II and LC3-II/LC3-I ratio. This increase of LC3-II/LC3-I was potently reversed by OKA treatment (Fig. 7E and F).

These data indicate that inhibition of PP2A by OKA reduces stress-induced autophagy regardless of the nature of the stress, indicating that PP2A might regulate common pathways of the molecular core machinery of autophagy.

3.6. OKA and PP2Ac knockdown activate both AMPK and mTORC1 signaling pathways

Exposure to OKA resulted in an increased phosphorylation of mTOR (at Ser2448 site) and AMPKα (at Thr172 site), and their activation as revealed by an increase of phosphorylation of their respective substrates P70S6K and acetyl CoA carboxylase (Fig. 8A and B). These results confirm previous data reported in hepatocytes and neurons (Samari et al., 2005; Yoon et al., 2008). Similar effects on mTOR and AMPK phosphorylation and activation were obtained following PP2Ac silencing. These data confirm

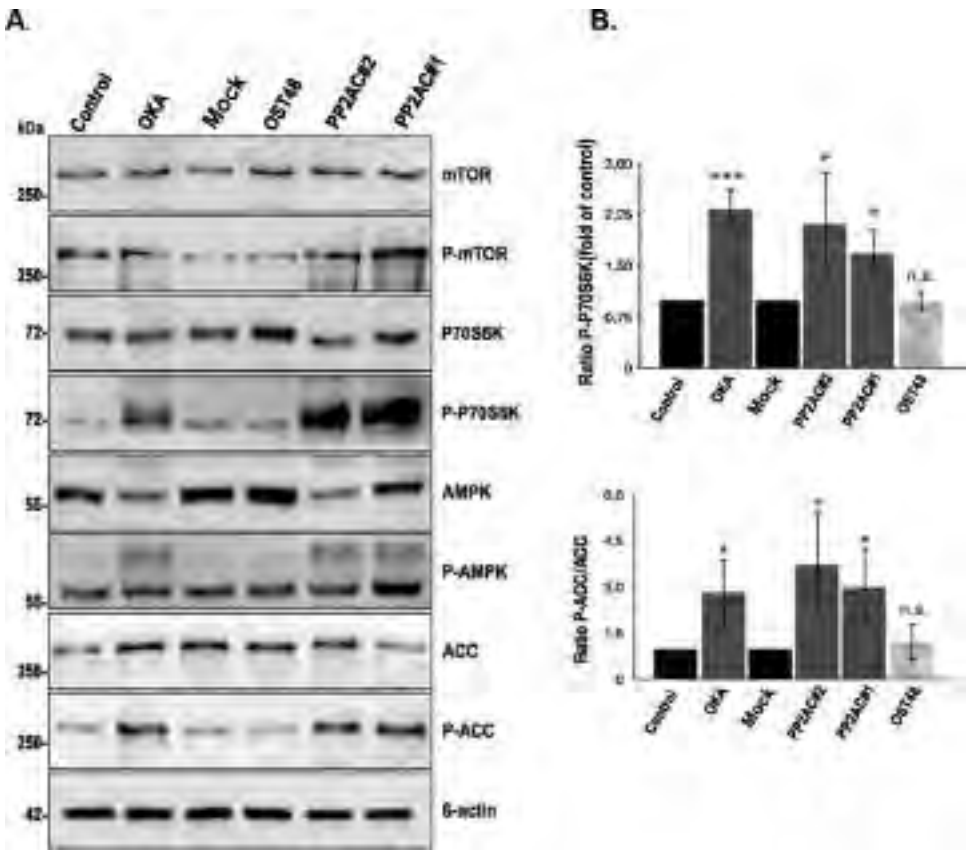

Fig. 8. Downregulation of protein phosphatase 2A (PP2A) activity either by okadaic acid (OKA) treatment or PP2A catalytic subunit (PP2Ac) knockdown activates mammalian target of rapamycin (mTOR) and AMP-activated kinase (AMPK) signaling pathways. Cultured neurons were either treated with 25 nM OKA, for 6 hours or subject to PP2Ac knockdown. OST48 silencing was used as a nonrelevant control. (A) Total cell lysates were immunoblotted for the detection of native and phosphorylated forms of mTOR, AMPK, and their respective substrates P70S6K and Acetyl CoA carboxylase (ACC) (see Table 1). (B) Semiquantitative analysis and calculation of the ratio of both native and phosphorylated forms of P70S6K and ACC are shown. β-actin was detected as a loading control. * $p < 0.05$; *** $p < 0.01$. Abbreviation: n.s., nonsignificant.

that OKA exerts its action on molecular components of the autophagy signaling pathways through the inhibition of PP2A, and that the inhibitory action on autophagy could result from mTOR activation. Moreover, as observed in hepatocytes, in our model of cultured neurons, AMPK might be implicated in the inhibition of autophagy, unless the putative positive action of AMPK on autophagy is overcome downstream of mTOR activation. This might indicate that PP2A might act downstream of AMPK on mTOR to regulate neuronal autophagy.

3.7. Inhibition of PP2A by OKA causes a relocalization of p62 to ubiquitin-positive inclusions

p62 is a multifunctional protein involved in cell death/survival, activation of transcription, and inflammation (Komatsu and Ichimura, 2010; Wooten et al., 2006). The PB-1 (Phox and Bhem1) domain in the N-terminus allows self-oligomerization of p62 and the C-termimal UBA (ubiquitin-associated) domain is responsible for p62 interaction with ubiquitinated proteins and aggresome formation. p62 also interacts through its LIR domain with LC3 and can be found in autophagosomes (Ichimura et al., 2008; Pankiv et al., 2007). p62 can be further degraded along with ubiquitinated proteins in autolysosomes. Consequently, suppression of autophagy leads to a marked accumulation of p62- and ubiquitin-positive protein inclusions. Such inclusions can be found in several neurodegenerative diseases; for example, p62 has been localized to ubiquitin-positive inclusions with tau aggregates in Alzheimer's disease (Babu et al., 2005; Komatsu and Ichimura, 2010; Kuusisto et al., 2008; Wooten et al., 2006). Therefore, as a result of the inhibition of autophagy, blockade of PP2A is expected to induce an accumulation of ubiquitinated protein aggregates positive for p62. In our cell culture model, p62 immunostaining showed that PP2A inactivation, either by OKA or by PP2Ac silencing, induced substantial relocalization of p62 from the cytosol, where staining of p62 is diffuse (except the presence of some p62-positive inclusions) in control neurons (tau-positive cells) (Fig. 9, control panel), to large rounded inclusion bodies in neurons where PP2A was blocked (Fig. 9, OKA and shRNA PP2Ac panels). The majority of these inclusions were positive for ubiquitin as shown by coim-

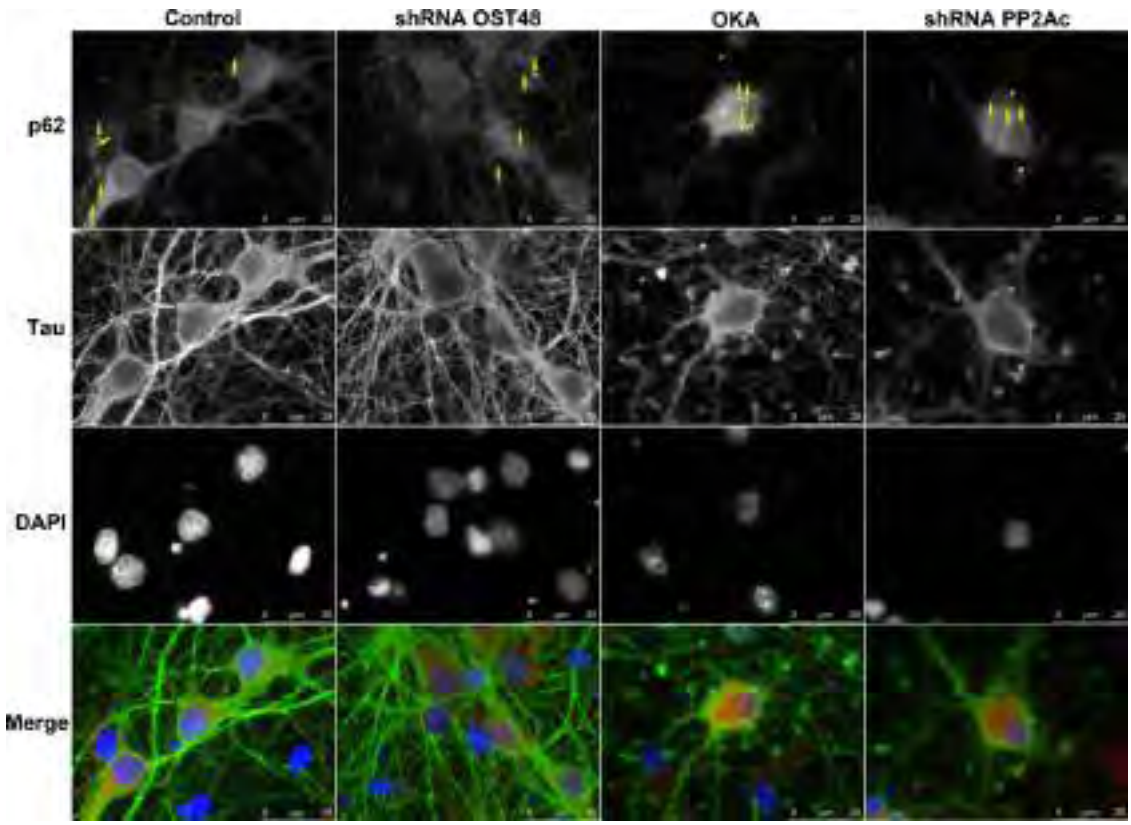

Fig. 9. Blockade of protein phosphatase 2A (PP2A) induces the accumulation of p62-positive inclusions in neurons. Cultured neurons were either treated with or without 25 nM okadaic acid (OKA) for 6 hours or subject to PP2A catalytic subunit (PP2Ac) knockdown. Intraneuronal p62-positive inclusions (arrows) were detected by dual immunofluorescence of p62 (red) and tau used as a neuronal marker (green). Cells were counterstained by the nuclear dye DAPI (blue). Immunofluorescence of p62 showed that PP2A blockade increased the number and the size of p62-positive inclusions (arrows) in neurons (tau-positive cells). Some of these inclusions showed colocalization of p62 and tau (arrowheads). Note that PP2A blockade dramatically impairs the neuronal cytoskeleton (neurite retraction and round-up of the cell body) as revealed by tau staining.

munostaining for ubiquitin and p62 (Fig. 10A). Dual-immunofluorescence staining for tau and p62 showed colocalization of p62 and tau in some of these protein inclusions (Fig. 9, see stainings for tau and p62 in panel OKA) and thus reproducing some neuropathological aspect of AD brain; besides, PP2A inactivation led to the disorganization of the neuronal cytoskeleton as manifested by the loss of tau staining in neurites and the formation of tau bundles in perikaryon around the nucleus and dystrophic neurites (Fig. 9, see tau staining in OKA and shRNA PP2Ac panels). Moreover, detection of ubiquitinated proteins by Western blot of ubiquitin revealed that blockade of PP2A activity, by OKA or by shRNA silencing of PP2Ac, resulted in an overall increase in protein ubiquitinylation (Fig. 10B). Cell fractionation into Triton-X100-soluble fraction (corresponding to the cytosolic fraction) and Triton-X100-insoluble fraction (which contains cytoskeleton, nuclei, membranes, and aggregates), and p62 Western blot detection, clearly showed that inhibition of PP2A by OKA, increased p62 in the insoluble fraction and concomitantly decreased it in the soluble fraction (Fig. 10C). These data confirm that p62 aggregates when PP2A was inhibited.

3.8. Inhibition of PP2A by OKA alters the distribution of LC3-I between the free cytosolic (detergent soluble) and bound (detergent-insoluble) fractions

The dynamics of microtubules is regulated by their interaction with MAPs. The MAP LC3 was originally isolated from the brain and was shown to interact with MAP1A and MAP1B heavy chains leading to an enhancement of the MAP1A and MAP1B binding to microtubules, indicating that LC3 can function as subunits of MAP1A and MAP1B polyproteins (Halpain and Dehmelt, 2006). LC3 binding to microtubules is mediated by ionic interaction of the N-terminus of LC3 with negatively charged tubulins of the outer side of microtubules. The C-terminus of LC3 primed by Atg4B (LC3-I) is responsible for the covalent attachment of LC3-I to the membrane of autophagosome. LC3 remains attached throughout autophagosome biogenesis, but is removed by Atg4 from the outer autophagosomal membrane before fusion with the lysosome (Mizushima et al., 2001). Through its LIR, p62 domain interacts with LC3 and targets polyubiquitinated protein aggregates to the nascent autophagosomes for further degradation by aggrephagy. So, to summarize, LC3-I can be found free in the

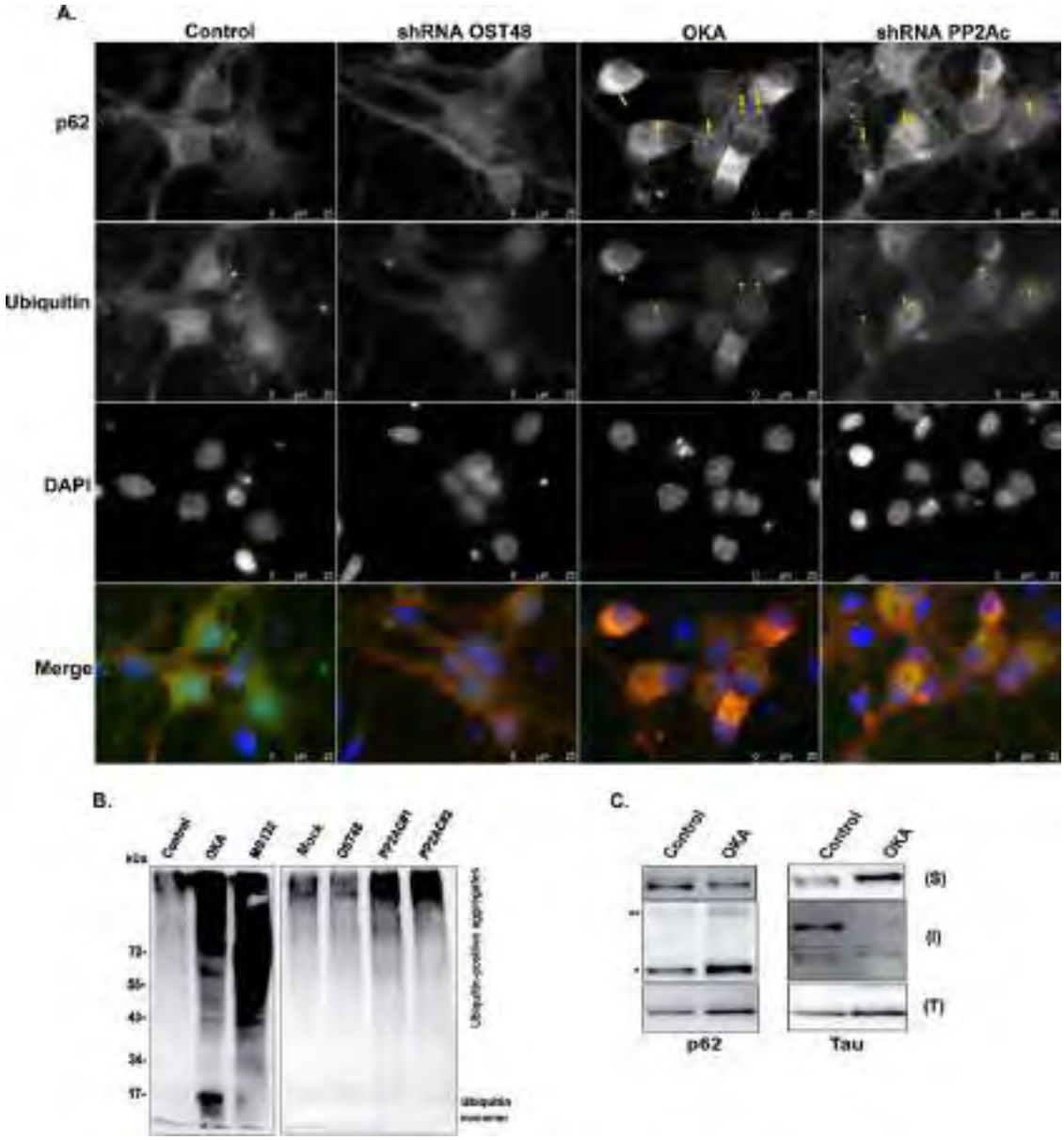

Fig. 10. Inhibition of protein phosphatase 2A (PP2A) leads to a relocalization of p62 to ubiquitin-containing bodies. (A) Colocalization of p62 and ubiquitin in the protein inclusions was revealed by coimmunostaining for p62 (red) and ubiquitin (green). Cells were counterstained by the nuclear dye DAPI (blue). Note that PP2A inhibition (by okadaic acid [OKA] or PP2A catalytic subunit [PP2Ac] silencing) increase the number of protein inclusions and virtually all of them were positive both for p62 (arrows) and ubiquitin (arrowheads) (B) Western blot analysis of protein ubiquitinylation following pharmacological or molecular inhibition of PP2A. Cultures exposed to MG132 were used as a positive control for ubiquitinated protein accumulation. (C) Western blot detection of p62 in Triton-X100-soluble (S) and -insoluble (I) fractions as well as in total (T) cell lysates. Tau detection was performed in order to validate the fractionation assay and to confirm the OKA-induced decrease of tau binding to microtubules. * Monomeric p62; ** This high molecular weight p62-immunopositive band might correspond to aggregated p62.

cytosol (Triton-soluble LC3), attached to microtubules or in complexes with different proteins like MAP, tubulin dimers, and p62 (Triton-insoluble LC3). Phosphorylation of MAP regulates their binding to microtubules. In neuronal cells, inhibition of PP2A resulted in hyperphosphorylation of the MAP tau, which becomes no longer able to bind microtubules (Rametti et al., 2004) and thereby results in the destabilization of neuronal microtubules. Therefore, we addressed the question of whether inhibition of PP2A alters or not LC3 binding to microtubules and more generally modifies its distribution between free and bound fractions. Consistent with previous findings (Xie et al., 2010), in control cultures (basal conditions), Western blot detection of LC3 showed that LC3-I was found both in Triton X-100-soluble and Triton X-100-insoluble fraction whereas LC3-II was mostly detected in Triton X-100-insoluble fraction. Treatment of cultured neurons with OKA

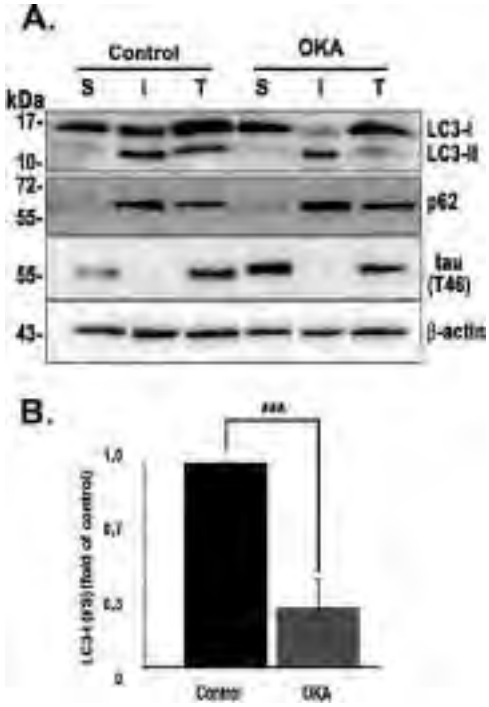

Fig. 11. Inhibition of protein phosphatase 2A (PP2A) by okadaic acid (OKA) impairs LC3-I distribution between Triton X-100-soluble and -insoluble fractions. Cultured neurons treated with or without 25 nM OKA were fractionated into Triton X-100-soluble (S) and Triton X-100-insoluble (I) fractions. Cell fractions were then immunoblotted for LC3, p62, tau, and β-actin used as a loading control. (A) Western blot detection of LC3, p62, tau, and β-actin. (B) Semiquantitative analysis of LC3 Western blots and calculation of ratio of LC3-I in fraction (I)/LC3-I in fraction (S). All data are representative of at least 3 independent experiments and were analyzed for statistical significance with Student t test. *** $p < 0.001$. Abbreviation: n.s., nonsignificant.

induced an increase LC3-I in Triton X-100-soluble fraction as determined by the calculation of the ratio insoluble/soluble LC3-I (Fig. 11A). The determination of the ratio insoluble/soluble LC3-I indicates that conversely to what observed for p62, exposure to OKA increased LC3-I in the soluble fraction and this increase was parallel to an LC3-I decrease in the insoluble fraction (Fig. 11B).

4. Discussion

We showed here that PP2A inactivation, either pharmacologically by OKA or by shRNA silencing of PP2A catalytic subunit inhibits autophagy at early stages before autophagosome maturation without directly affecting the proper function of lysosomes. Komatsu and colleagues (2007b) discriminate constitutive autophagy with homeostatic function from autophagy induced by various cellular stresses compromising the integrity of the proteome. This is a very important parameter in nondividing cells such as neurons (Komatsu et al., 2007b). In our study, blockade of PP2A inhibits not only basal autophagy, but also autophagy induced in cell stress conditions including glucose and serum deprivation, mTOR inhibition by rapamycin, ER stress induction by tunicamycin, and UPS inhibition by MG132. These data indicate that blockade of PP2A downregulates autophagy by acting at convergent signaling pathways involved in the control of the autophagy core machinery. In fact, blockade of PP2A activates mTOR pathway, which negatively regulates this machinery. Importantly, suppression of PP2A activity resulted in the accumulation of ubiquitinated proteins, which is correlated with intraneuronal accumulation of p62- and ubiquitin-positive inclusions, likely as a consequence of autophagy downregulation. These data are consistent with previous findings in mouse, showing that specific invalidation of autophagy in the nervous system resulted in the accumulation of ubiquitin-positive and p62-positive inclusions (Hara et al., 2006; Komatsu et al., 2006, 2007b; Korolchuk et al., 2009). Therefore, our findings provide links between PP2A downregulation, autophagy inhibition and protein aggregation, and are relevant to human neurodegenerative diseases, especially AD where PP2A is downregulated, autophagy is disrupted, and ubiquitinated protein inclusions are found (Babu et al., 2005; Komatsu and Ichimura, 2010; Kuusisto et al., 2008; Wooten et al., 2006).

PP2A is able to regulate the phosphorylation of numerous substrates and likely among them, some like mTOR pathway components are molecular targets upstream of the autophagy core machinery. It is noteworthy mentioning that an increase in mTOR phosphorylation and activation was reported in AD brains (Griffin et al., 2005) and PP2A can be activated by rapamycin (Park et al., 2008). Until now, PP2A was considered to have a permissive effect upon autophagy, but no data as yet implicate directly PP2A in the autophagy signaling pathways. In our study, rapamycin failed to reverse OKA-induced decrease of autophagy indicating that either rapamycin or OKA act noncompetitively on the mTOR pathway or PP2A acts downstream of mTOR during the autophagy process, and PP2A might possibly exert a negative feedback upon mTOR. This possibility is sustained by a recent study conducted by Liu et al. (2011), showing that perturbation in MID1 (E3 ligase)/PP2A axis affects mTORC1 signaling and especially increased PP2Ac levels caused by the UPS inhibition led to the disruption of the mTOR/Raptor complex and therefore to the downregulation of mTORC1 signaling.

PP2A might also regulate neuronal autophagy by affecting AMPK, which acts upstream of mTOR. In mammalian cells, a conflicting role of AMPK in autophagy has been reported: some studies demonstrated that AMPK is a trigger of autophagy in cell lines and primary cultured neurons (Liang et al., 2007; Meley et al., 2006; Vingtdeux et al., 2010a, 2010b), while there is evidence indicating that activation of AMPK, which can be achieved by OKA, suppresses autophagy in hepatocytes (Samari and Seglen, 1998; Samari et al., 2005). A recent study demonstrated that autophagy can be induced under low glucose concentration in

mouse embryonic fibroblast cells lacking AMPKα (Williams et al., 2009). Our findings showed that, despite the activation of AMPK, PP2A blockade negatively regulates neuronal autophagy, which is consistent with data obtained in hepatocytes. These data indicate that PP2A regulates neuronal autophagy downstream of AMPK.

Treatment with OKA is used as a model for neurodegeneration both in vivo and in cell culture models. Induction of autophagy (by rapamycin) was reported to be neuroprotective (Ravikumar et al., 2004, 2006; Young et al., 2009; Zhang et al., 2008). Whether inhibition of autophagy, due to the downregulation of PP2A, is causal or not of protein aggregation and neurodegeneration remains to be determined. In our study, because rapamycin failed to restore a normal level of autophagy sustains the possibility that PP2A may act downstream of mTOR and/or prevent the action of rapamycin on the formation mTORC1. Therefore, protection against OKA-induced neuronal death by activating mTOR-independent autophagy should be envisaged (Krüger et al., 2012).

A concern can be legitimately raised by the use of the inhibition PP2A for studying the autophagy process because PP2A regulates the phosphorylation of many substrates involved in various cell functions. As mentioned above, blockade of PP2A resulted in the phosphorylation of all protein substrates examined here, especially that of key kinases involved in metabolism and autophagy signaling: mTOR and AMPK and their respective substrates, p70S6K and acetyl CoA carboxylase confirming their activation, but, it is not certain that impairment of mTOR and AMPK pathways are the sole mechanism responsible for the autophagy downregulation induced by the blockade of PP2A. An AMPK- and mTOR-independent control of autophagy by PP2A might also be possible; for example, through its action on the components of the autophagy core machinery could also be involved. In addition, it is interesting to mention that MAP1-LC3 phosphorylation by protein kinase C (Jiang et al., 2010) or protein kinase A (Cherra et al., 2010) resulted in the inhibition of autophagy. Because PP2A regulates the phosphorylation of numerous substrates in the cell, it will be interesting to determine whether or not LC3 is a PP2A substrate, and how LC3 phosphorylation affects neuronal autophagy in our cell model. In other words, does increased phosphorylation of LC3 impair its attachment to phosphatidyl ethanolamine of nascent autophagosomal membrane? This would explain the decrease in LC3-I to LC3-II conversion and the in situ increase in the cytosolic LC3 (LC3-I isoform) under conditions of PP2A inhibition. Does a putative LC3 phosphorylation impair its interaction with other proteins (in complexes with LC3) or microtubules and thereby explaining the OKA-induced distribution of LC3-I between the free and the bound fractions? Thus, the role of PP2A in the regulation of LC3 phosphorylation and its impact on the autophagy process should be analyzed.

Microtubules are involved throughout the autophagy process from initiation of autophagosome formation (Di Bartolomeo et al., 2010) to fusion of autophagosomes with lysosomes. On the other hand, microtubules constitute an essential component of neuronal cytoskeleton maintaining neuronal polarity through their stabilization by MAPs (Perez, 2009). Increased phosphorylation (that can result from the inhibition of PP2A) of MAPs impairs their binding to microtubules and thereby leads to the destabilization of the neuronal cytoskeleton. In neurons, LC3-I redistributes to neurites from a mainly perikaryal location (Nixon, 2007; Yu et al., 2005) and autophagosome biogenesis seems to mainly take place at the synaptic compartment (Nixon, 2007). Therefore, under conditions of PP2A inhibition, it is possible that destabilization of microtubules and the loss of LC3 binding to microtubules might impair LC3-I anterograde transport. Consequently, LC3-I accumulates in the cytosol of neuronal cell bodies and autophagosome biogenesis at the axonal and synaptic compartments is indirectly blocked. Therefore, the implication of a neuronal cytoskeleton destabilization in the downregulation of autophagy should be determined in our neuronal cell model.

Reports from Nixon's group showed that in AD brains exhibited a marked accumulation of immature autophagic vacuoles, especially a build up of autophagosomes in dystrophic neurites (Nixon et al., 2005). It was suggested that this massive accumulation of immature AV in dystrophic neurites could result from an impairment of autophagosome retrograde transport, which is microtubule-dependent, and thus preventing autophagosome maturation to autolysosome and finally interfering with the neuroprotective function of autophagy (Nixon et al., 2005). So, how can we reconcile these data from AD brains with our findings in cultured neurons where we rather observed an overall decrease in autophagosome biogenesis? Because our in situ quantification of autophagosomes was only performed in perikarya because we used high cell density cultures with a developed neurite network making it difficult to assess autophagosomes in neuronal processes, we cannot rule out the possibility that localized autophagosome accumulation in the dendrites and axons can take place. Another possibility is that autophagosome accumulation in AD brains might represent a positive feedback as a consequence of an initial long-term inhibition of autophagy in this chronic human disease. This possibility cannot be tested in our model because long-term inhibition of PP2A is highly deleterious for neurons and it is not guaranteed that the possible resulting disruption of autophagy is not secondary to neuronal death.

In conclusion, despite a myriad of actions of PP2A in the cell, our study provide however direct evidence that in vitro downregulation of PP2A inhibits autophagy and leads to intraneuronal accumulation of protein inclusions, a neuropathological feature of several neurodegenerative diseases. The specific molecular mechanisms responsible for the ac-

tion of PP2A on autophagy remain to be determined. Moreover, the important question of whether inhibition of autophagy contributes or not to neuronal death induced by the blockade of PP2A remains to be answered. If it appears that inhibition of autophagy by the blockade of PP2A is responsible for neuronal death, finding drugs that permit the recovery of (or reasonably increase) autophagic activity in this model will be of therapeutic interest.

Disclosure statement

The authors declare no conflicts of interest.

Acknowledgements

This work was supported by a grant from the Association of "France Alzheimer" and related disorders' (Ph.D. fellowship for AM), the French Ministry of Education and Research, the "Région Limousin," The LECMA) association (Ligue Européenne Contre la Maladie d'Alzheimer). The authors thank Dr. Judith Haendeler, University of Frankfurt for providing us with the PP2Ac construct, and Mrs. Marie-Laure Perrin and Miss Estelle Touraille for their technical assistance.

Appendix A. Supplementary data

Supplementary data associated with this article can be found, in the online version, at http://dx.doi.org/10.1016/j.neurobiolaging.2012.06.026.

References

Babu, J.R., Geetha, T., Wooten, M.W., 2005. Sequestosome 1/p62 shuttles polyubiquitinated tau for proteasomal degradation. J. Neurochem. 94, 192–203.

Bauvy, C., Meijer, A.J., Codogno, P., 2009. Assaying of autophagic protein degradation. Methods Enzymol. 452, 47–61.

Berger, Z., Ravikumar, B., Menzies, F.M., Oroz, L.G., Underwood, B.R., Pangalos, M.N., Schmitt, I., Wullner, U., Evert, B.O., O'Kane, C.J., Rubinsztein, D.C., 2006. Rapamycin alleviates toxicity of different aggregate-prone proteins. Hum. Mol. Genet. 15, 433–442.

Bjørkøy, G., Lamark, T., Brech, A., Outzen, H., Perander, M., Overvatn, A., Stenmark, H., Johansen, T., 2005. p62/SQSTM1 forms protein aggregates degraded by autophagy and has a protective effect on huntingtin-induced cell death. J. Cell Biol. 171, 603–614.

Boland, B., Kumar, A., Lee, S., Platt, F.M., Wegiel, J., Yu, W.H., Nixon, R.A., 2008. Autophagy induction and autophagosome clearance in neurons: relationship to autophagic pathology in Alzheimer's disease. J. Neurosci. 28, 6926–6937.

Cataldo, A.M., Hamilton, D.J., Barnett, J.L., Paskevich, P.A., Nixon, R.A., 1996. Abnormalities of the endosomal-lysosomal system in Alzheimer's disease: relationship to disease pathogenesis. Adv. Exp. Med. Biol. 389, 271–280.

Chen, J., Peterson, R.T., Schreiber, S.L., 1998. Alpha 4 associates with protein phosphatases 2A, 4, and 6. Biochem. Biophys. Res. Commun. 247, 827–832.

Chen, S., Li, B., Grundke-Iqbal, I., Iqbal, K., 2008. I1PP2A affects tau phosphorylation via association with the catalytic subunit of protein phosphatase 2A. J. Biol. Chem. 283, 10513–10521.

Cherra, S.J., 3rd, Kulich, S.M., Uechi, G., Balasubramani, M., Mountzouris, J., Day, B.W., Chu, C.T., 2010. Regulation of the autophagy protein LC3 by phosphorylation. J. Cell Biol. 190, 533–539.

Codogno, P., Meijer, A.J., 2005. Autophagy and signaling: their role in cell survival and cell death. Cell Death Differ. 12, 1509–1518.

Di Bartolomeo, S., Corazzari, M., Nazio, F., Oliverio, S., Lisi, G., Antonioli, M., Pagliarini, V., Matteoni, S., Fuoco, C., Giunta, L., D'Amelio, M., Nardacci, R., Romagnoli, A., Piacentini, M., Cecconi, F., Fimia, G.M., 2010. The dynamic interaction of AMBRA1 with the dynein motor complex regulates mammalian autophagy. J. Cell Biol. 191, 155–168.

Ding, W.X., Ni, H.M., Gao, W., Yoshimori, T., Stolz, D.B., Ron, D., Yin, X.M., 2007. Linking of autophagy to ubiquitin-proteasome system is important for the regulation of endoplasmic reticulum stress and cell viability. Am. J. Pathol. 171, 513–524.

Fogarty, S., Hardie, D.G., 2010. Development of protein kinase activators: AMPK as a target in metabolic disorders and cancer. Biochim. Biophys. Acta 1804, 581–591.

Fujiki, H., Suganuma, M., 1993. Tumor promotion by inhibitors of protein phosphatases 1 and 2A: the okadaic acid class of compounds. Adv. Cancer Res. 61, 143–194.

Gong, C.X., Singh, T.J., Grundke-Iqbal, I., Iqbal, K., 1993. Phosphoprotein phosphatase activities in Alzheimer disease brain. J. Neurochem. 61, 921–927.

Griffin, R.J., Moloney, A., Kelliher, M., Johnston, J.A., Ravid, R., Dockery, P., O'Connor, R., O'Neill, C., 2005. Activation of Akt/PKB, increased phosphorylation of Akt substrates and loss and altered distribution of Akt and PTEN are features of Alzheimer's disease pathology. J. Neurochem. 93, 105–117.

Halpain, S., Dehmelt, L., 2006. The MAP1 family of microtubule-associated proteins. Genome Biol. 7, 224.

Hara, T., Nakamura, K., Matsui, M., Yamamoto, A., Nakahara, Y., Suzuki-Migishima, R., Yokoyama, M., Mishima, K., Saito, I., Okano, H., Mizushima, N., 2006. Suppression of basal autophagy in neural cells causes neurodegenerative disease in mice. Nature 441, 885–889.

Hetz, C., Thielen, P., Matus, S., Nassif, M., Court, F., Kiffin, R., Martinez, G., Cuervo, A.M., Brown, R.H., Glimcher, L.H., 2009. XBP-1 deficiency in the nervous system protects against amyotrophic lateral sclerosis by increasing autophagy. Genes Dev. 23, 2294–2306.

Holen, I., Gordon, P.B., Seglen, P.O., 1993. Inhibition of hepatocytic autophagy by okadaic acid and other protein phosphatase inhibitors. Eur. J. Biochem. 215, 113–122.

Ichimura, Y., Kirisako, T., Takao, T., Satomi, Y., Shimonishi, Y., Ishihara, N., Mizushima, N., Tanida, I., Kominami, E., Ohsumi, M., Noda, T., Ohsumi, Y., 2000. A ubiquitin-like system mediates protein lipidation. Nature 408, 488–492.

Ichimura, Y., Kominami, E., Tanaka, K., Komatsu, M., 2008. Selective turnover of p62/A170/SQSTM1 by autophagy. Autophagy 4, 1063–1066.

Jiang, H., Cheng, D., Liu, W., Peng, J., Feng, J., 2010. Protein kinase C inhibits autophagy and phosphorylates LC3. Biochem. Biophys. Res. Commun. 395, 471–476.

Kabeya, Y., Mizushima, N., Ueno, T., Yamamoto, A., Kirisako, T., Noda, T., Kominami, E., Ohsumi, Y., Yoshimori, T., 2000. LC3, a mammalian homologue of yeast Apg8p, is localized in autophagosome membranes after processing. EMBO J. 19, 5720–5728.

Kanzawa, T., Zhang, L., Xiao, L., Germano, I.M., Kondo, Y., Kondo, S., 2005. Arsenic trioxide induces autophagic cell death in malignant glioma cells by upregulation of mitochondrial cell death protein BNIP3. Oncogene 24, 980–991.

Kaushik, S., Massey, A.C., Mizushima, N., Cuervo, A.M., 2008. Constitutive activation of chaperone-mediated autophagy in cells with impaired macroautophagy. Mol. Biol. Cell 19, 2179–2192.

Kimura, S., Noda, T., Yoshimori, T., 2008. Dynein-dependent movement of autophagosomes mediates efficient encounters with lysosomes. Cell Struct. Funct. 33, 109–122.

Knaevelsrud, H., Simonsen, A., 2010. Fighting disease by selective autophagy of aggregate-prone proteins. FEBS Lett. 584, 2635–2645.

Komatsu, M., Ichimura, Y., 2010. Physiological significance of selective degradation of p62 by autophagy. FEBS Lett. 584, 1374–1378.

Komatsu, M., Ueno, T., Waguri, S., Uchiyama, Y., Kominami, E., Tanaka, K., 2007a. Constitutive autophagy: vital role in clearance of unfavorable proteins in neurons. Cell Death Differ. 14, 887–894.

Komatsu, M., Waguri, S., Chiba, T., Murata, S., Iwata, J., Tanida, I., Ueno, T., Koike, M., Uchiyama, Y., Kominami, E., Tanaka, K., 2006. Loss of autophagy in the central nervous system causes neurodegeneration in mice. Nature 441, 880–884.

Komatsu, M., Waguri, S., Koike, M., Sou, Y.S., Ueno, T., Hara, T., Mizushima, N., Iwata, J., Ezaki, J., Murata, S., Hamazaki, J., Nishito, Y., Iemura, S., Natsume, T., Yanagawa, T., Uwayama, J., Warabi, E., Yoshida, H., Ishii, T., Kobayashi, A., Yamamoto, M., Yue, Z., Uchiyama, Y., Kominami, E., Tanaka, K., 2007b. Homeostatic levels of p62 control cytoplasmic inclusion body formation in autophagy-deficient mice. Cell 131, 1149–1163.

Korolchuk, V.I., Menzies, F.M., Rubinsztein, D.C., 2009. A novel link between autophagy and the ubiquitin-proteasome system. Autophagy 5, 862–863.

Krüger, U., Wang, Y., Kumar, S., Mandelkow, E.M., 2012. Autophagic degradation of tau in primary neurons and its enhancement by trehalose. Neurobiol. Aging 33, 2291–2305.

Kuma, A., Matsui, M., Mizushima, N., 2007. LC3, an autophagosome marker, can be incorporated into protein aggregates independent of autophagy: caution in the interpretation of LC3 localization. Autophagy 3, 323–328.

Kuusisto, E., Kauppinen, T., Alafuzoff, I., 2008. Use of p62/SQSTM1 antibodies for neuropathological diagnosis. Neuropathol. Appl. Neurobiol. 34, 169–180.

Lee, S., Sato, Y., Nixon, R.A., 2011. Lysosomal proteolysis inhibition selectively disrupts axonal transport of degradative organelles and causes an Alzheimer's-like axonal dystrophy. J. Neurosci. 31, 7817–7830.

Lépine, S., Allegood, J.C., Park, M., Dent, P., Milstien, S., Spiegel, S., 2011. Sphingosine-1-phosphate phosphohydrolase-1 regulates ER stress-induced autophagy. Cell Death Differ. 18, 350–361.

Liang, J., Shao, S.H., Xu, Z.X., Hennessy, B., Ding, Z., Larrea, M., Kondo, S., Dumont, D.J., Gutterman, J.U., Walker, C.L., Slingerland, J.M., Mills, G.B., 2007. The energy sensing LKB1-AMPK pathway regulates p27(kip1) phosphorylation mediating the decision to enter autophagy or apoptosis. Nat. Cell Biol. 9, 218–224.

Liu, E., Knutzen, C.A., Krauss, S., Schweiger, S., Chiang, G.G., 2011. Control of mTORC1 signaling by the Opitz syndrome protein MID1. Proc. Natl. Acad. Sci. U. S. A. 108, 8680–8685.

Liu, F., Grundke-Iqbal, I., Iqbal, K., Gong, C.X., 2005. Contributions of protein phosphatases PP1, PP2A, PP2B and PP5 to the regulation of tau phosphorylation. Eur. J. Neurosci. 22, 1942–1950.

Martin, L., Magnaudeix, A., Esclaire, F., Yardin, C., Terro, F., 2009. Inhibition of glycogen synthase kinase-3beta downregulates total tau proteins in cultured neurons and its reversal by the blockade of protein phosphatase-2A. Brain Res. 1252, 66–75.

Meley, D., Bauvy, C., Houben-Weerts, J.H., Dubbelhuis, P.F., Helmond, M.T., Codogno, P., Meijer, A.J., 2006. AMP-activated protein kinase and the regulation of autophagic proteolysis. J. Biol. Chem. 281, 34870–34879.

Midorikawa, R., Yamamoto-Hino, M., Awano, W., Hinohara, Y., Suzuki, E., Ueda, R., Goto, S., 2010. Autophagy-dependent rhodopsin degradation prevents retinal degeneration in Drosophila. J. Neurosci. 30, 10703–10719.

Mizushima, N., Levine, B., Cuervo, A.M., Klionsky, D.J., 2008. Autophagy fights disease through cellular self-digestion. Nature 451, 1069–1075.

Mizushima, N., Yamamoto, A., Hatano, M., Kobayashi, Y., Kabeya, Y., Suzuki, K., Tokuhisa, T., Ohsumi, Y., Yoshimori, T., 2001. Dissection of autophagosome formation using Apg5-deficient mouse embryonic stem cells. J. Cell Biol. 152, 657–668.

Mizushima, N., Yoshimori, T., 2007. How to interpret LC3 immunoblotting. Autophagy 3, 542–545.

Morimoto, N., Nagai, M., Ohta, Y., Miyazaki, K., Kurata, T., Morimoto, M., Murakami, T., Takehisa, Y., Ikeda, Y., Kamiya, T., Abe, K., 2007. Increased autophagy in transgenic mice with a G93A mutant SOD1 gene. Brain Res. 1167, 112–117.

Nanahoshi, M., Nishiuma, T., Tsujishita, Y., Hara, K., Inui, S., Sakaguchi, N., Yonezawa, K., 1998. Regulation of protein phosphatase 2A catalytic activity by alpha4 protein and its yeast homolog Tap42. Biochem. Biophys. Res. Commun. 251, 520–526.

Ni, H.M., Bockus, A., Wozniak, A.L., Jones, K., Weinman, S., Yin, X.M., Ding, W.X., 2011. Dissecting the dynamic turnover of GFP-LC3 in the autolysosome. Autophagy 7, 188–204.

Nijholt, D.A., de Graaf, T.R., van Haastert, E.S., Oliveira, A.O., Berkers, C.R., Zwart, R., Ovaa, H., Baas, F., Hoozemans, J.J., Scheper, W., 2011. Endoplasmic reticulum stress activates autophagy but not the proteasome in neuronal cells: implications for Alzheimer's disease. Cell Death Differ. 18, 1071–1081.

Nixon, R.A., 2006. Autophagy in neurodegenerative disease: friend, foe or turncoat? Trends Neurosci. 29, 528–535.

Nixon, R.A., 2007. Autophagy, amyloidogenesis and Alzheimer disease. J. Cell Sci. 120, 4081–4091.

Nixon, R.A., Cataldo, A.M., Mathews, P.M., 2000. The endosomal-lysosomal system of neurons in Alzheimer's disease pathogenesis: a review. Neurochem. Res. 25, 1161–1172.

Nixon, R.A., Wegiel, J., Kumar, A., Yu, W.H., Peterhoff, C., Cataldo, A., Cuervo, A.M., 2005. Extensive involvement of autophagy in Alzheimer disease: an immuno-electron microscopy study. J. Neuropathol. Exp. Neurol. 64, 113–122.

Ogata, M., Hino, S., Saito, A., Morikawa, K., Kondo, S., Kanemoto, S., Murakami, T., Taniguchi, M., Tanii, I., Yoshinaga, K., Shiosaka, S., Hammarback, J.A., Urano, F., Imaizumi, K., 2006. Autophagy is activated for cell survival after endoplasmic reticulum stress. Mol. Cell. Biol. 26, 9220–9231.

Pandey, U.B., Nie, Z., Batlevi, Y., McCray, B.A., Ritson, G.P., Nedelsky, N.B., Schwartz, S.L., DiProspero, N.A., Knight, M.A., Schuldiner, O., Padmanabhan, R., Hild, M., Berry, D.L., Garza, D., Hubbert, C.C., Yao, T.P., Baehrecke, E.H., Taylor, J.P., 2007. HDAC6 rescues neurodegeneration and provides an essential link between autophagy and the UPS. Nature 447, 859–863.

Pankiv, S., Clausen, T.H., Lamark, T., Brech, A., Bruun, J.A., Outzen, H., Øvervatn, A., Bjørkøy, G., Johansen, T., 2007. p62/SQSTM1 binds directly to Atg8/LC3 to facilitate degradation of ubiquitinated protein aggregates by autophagy. J. Biol. Chem. 282, 24131–24145.

Park, I.H., Yeum, C.E., Chae, G.T., Lee, S.B., 2008. Effect of rifampicin to inhibit rapamycin-induced autophagy via the suppression of protein phosphatase 2A activity. Immunopharmacol. Immunotoxicol. 30, 837–849.

Perez, E.A., 2009. Microtubule inhibitors: differentiating tubulin-inhibiting agents based on mechanisms of action, clinical activity, and resistance. Mol. Cancer Ther. 8, 2086–2095.

Pickford, F., Masliah, E., Britschgi, M., Lucin, K., Narasimhan, R., Jaeger, P.A., Small, S., Spencer, B., Rockenstein, E., Levine, B., Wyss-Coray, T., 2008. The autophagy-related protein beclin 1 shows reduced expression in early Alzheimer disease and regulates amyloid beta accumulation in mice. J. Clin. Invest. 118, 2190–2199.

Prickett, T.D., Brautigan, D.L., 2006. The alpha4 regulatory subunit exerts opposing allosteric effects on protein phosphatases PP6 and PP2A. J. Biol. Chem. 281, 30503–30511.

Rametti, A., Esclaire, F., Yardin, C., Terro, F., 2004. Linking alterations in tau phosphorylation and cleavage during neuronal apoptosis. J. Biol. Chem. 279, 54518–54528.

Ravikumar, B., Berger, Z., Vacher, C., O'Kane, C.J., Rubinsztein, D.C., 2006. Rapamycin pre-treatment protects against apoptosis. Hum. Mol. Genet. 15, 1209–1216.

Ravikumar, B., Vacher, C., Berger, Z., Davies, J.E., Luo, S., Oroz, L.G., Scaravilli, F., Easton, D.F., Duden, R., O'Kane, C.J., Rubinsztein, D.C., 2004. Inhibition of mTOR induces autophagy and reduces toxicity of polyglutamine expansions in fly and mouse models of Huntington disease. Nat. Genet. 36, 585–595.

Rideout, H.J., Lang-Rollin, I., Stefanis, L., 2004. Involvement of macroautophagy in the dissolution of neuronal inclusions. Int. J. Biochem. Cell Biol. 36, 2551–2562.

Rubinsztein, D.C., 2007. Autophagy induction rescues toxicity mediated by proteasome inhibition. Neuron 54, 854–856.

Rubinsztein, D.C., Nixon, R.A., 2010. Rapamycin induces autophagic flux in neurons. Proc. Natl. Acad. Sci. U. S. A. 107, E181.

Samari, H.R., Møller, M.T., Holden, L., Asmyhr, T., Seglen, P.O., 2005. Stimulation of hepatocytic AMP-activated protein kinase by okadaic acid and other autophagy-suppressive toxins. Biochem. J. 386, 237–244.

Samari, H.R., Seglen, P.O., 1998. Inhibition of hepatocytic autophagy by adenosine, aminoimidazole-4-carboxamide riboside, and N6-mercaptopurine riboside. Evidence for involvement of amp-activated protein kinase. J. Biol. Chem. 273, 23758–23763.

Sarkar, S., Davies, J.E., Huang, Z., Tunnacliffe, A., Rubinsztein, D.C., 2007. Trehalose, a novel mTOR-independent autophagy enhancer, accelerates the clearance of mutant huntingtin and alpha-synuclein. J. Biol. Chem. 282, 5641–5652.

Sarkar, S., Floto, R.A., Berger, Z., Imarisio, S., Cordenier, A., Pasco, M., Cook, L.J., Rubinsztein, D.C., 2005. Lithium induces autophagy by inhibiting inositol monophosphatase. J. Cell Biol. 170, 1101–1111.

Sarkar, S., Ravikumar, B., Floto, R.A., Rubinsztein, D.C., 2009. Rapamycin and mTOR-independent autophagy inducers ameliorate toxicity of polyglutamine-expanded huntingtin and related proteinopathies. Cell Death Differ. 16, 46–56.

Seglen, P.O., Øverbye, A., Saetre, F., 2009. Sequestration assays for mammalian autophagy. Methods Enzymol. 452, 63–83.

Seubert, P., Mawal-Dewan, M., Barbour, R., Jakes, R., Goedert, M., Johnson, G.V., Litersky, J.M., Schenk, D., Lieberburg, I., Trojanowski, J.Q., etAl, etA.l, 1995. Detection of phosphorylated Ser262 in fetal tau, adult tau, and paired helical filament tau. J. Biol. Chem. 270, 18917–18922.

Shintani, T., Yamazaki, F., Katoh, T., Umekawa, M., Matahira, Y., Hori, S., Kakizuka, A., Totani, K., Yamamoto, K., Ashida, H., 2010. Glucosamine induces autophagy via an mTOR-independent pathway. Biochem. Biophys. Res. Commun. 391, 1775–1779.

Sontag, E., Nunbhakdi-Craig, V., Sontag, J.M., Diaz-Arrastia, R., Ogris, E., Dayal, S., Lentz, S.R., Arning, E., Bottiglieri, T., 2007. Protein phosphatase 2A methyltransferase links homocysteine metabolism with tau and amyloid precursor protein regulation. J. Neurosci. 27, 2751–2759.

Tanida, I., Ueno, T., Kominami, E., 2004. Human light chain 3/MAP1LC3B is cleaved at its carboxyl-terminal Met121 to expose Gly120 for lipidation and targeting to autophagosomal membranes. J. Biol. Chem. 279, 47704–47710.

Tanimukai, H., Grundke-Iqbal, I., Iqbal, K., 2005. Up-regulation of inhibitors of protein phosphatase-2A in Alzheimer's disease. Am. J. Pathol. 166, 1761–1771.

Trockenbacher, A., Suckow, V., Foerster, J., Winter, J., Krauss, S., Ropers, H.H., Schneider, R., Schweiger, S., 2001. MID1, mutated in Opitz syndrome, encodes an ubiquitin ligase that targets phosphatase 2A for degradation. Nat. Genet. 29, 287–294.

Vingtdeux, V., Chandakkar, P., Zhao, H., d'Abramo, C., Davies, P., Marambaud, P., 2010a. Novel synthetic small-molecule activators of AMPK as enhancers of autophagy and amyloid-beta peptide degradation. FASEB J. 25, 219–231.

Vingtdeux, V., Giliberto, L., Zhao, H., Chandakkar, P., Wu, Q., Simon, J.E., Janle, E.M., Lobo, J., Ferruzzi, M.G., Davies, P., Marambaud, P., 2010b. AMP-activated protein kinase signaling activation by resveratrol modulates amyloid-beta peptide metabolism. J. Biol. Chem. 285, 9100–9113.

Vogelsberg-Ragaglia, V., Schuck, T., Trojanowski, J.Q., Lee, V.M., 2001. PP2A mRNA expression is quantitatively decreased in Alzheimer's disease hippocampus. Exp. Neurol. 168, 402–412.

Webb, J.L., Ravikumar, B., Atkins, J., Skepper, J.N., Rubinsztein, D.C., 2003. Alpha-Synuclein is degraded by both autophagy and the proteasome. J. Biol. Chem. 278, 25009–25013.

Williams, A., Sarkar, S., Cuddon, P., Ttofi, E.K., Saiki, S., Siddiqi, F.H., Jahreiss, L., Fleming, A., Pask, D., Goldsmith, P., O'Kane, C.J., Floto, R.A., Rubinsztein, D.C., 2008. Novel targets for Huntington's disease in an mTOR-independent autophagy pathway. Nat. Chem. Biol. 4, 295–305.

Williams, T., Brenman, J.E., 2008. LKB1 and AMPK in cell polarity and division. Trends Cell Biol. 18, 193–198.

Williams, T., Forsberg, L.J., Viollet, B., Brenman, J.E., 2009. Basal autophagy induction without AMP-activated protein kinase under low glucose conditions. Autophagy 5, 1155–1165.

Wooten, M.W., Hu, X., Babu, J.R., Seibenhener, M.L., Geetha, T., Paine, M.G., Wooten, M.C., 2006. Signaling, polyubiquitination, trafficking, and inclusions: sequestosome 1/p62's role in neurodegenerative disease. J. Biomed. Biotechnol. 2006, 62079.

Xie, R., Nguyen, S., McKeehan, W.L., Liu, L., 2010. Acetylated microtubules are required for fusion of autophagosomes with lysosomes. BMC Cell Biol. 11, 89.

Xu, Y., Chen, Y., Zhang, P., Jeffrey, P.D., Shi, Y., 2008. Structure of a protein phosphatase 2A holoenzyme: insights into B55-mediated Tau dephosphorylation. Mol. Cell 31, 873–885.

Yoon, S.Y., Choi, J.E., Kweon, H.S., Choe, H., Kim, S.W., Hwang, O., Lee, H., Lee, J.Y., Kim, D.H., 2008. Okadaic acid increases autophagosomes in rat neurons: implications for Alzheimer's disease. J. Neurosci. Res. 86, 3230–3239.

Yorimitsu, T., He, C., Wang, K., Klionsky, D.J., 2009. Tap42-associated protein phosphatase type 2A negatively regulates induction of autophagy. Autophagy 5, 616–624.

Yorimitsu, T., Nair, U., Yang, Z., Klionsky, D.J., 2006. Endoplasmic reticulum stress triggers autophagy. J. Biol. Chem. 281, 30299–30304.

Young, J.E., Martinez, R.A., La Spada, A.R., 2009. Nutrient deprivation induces neuronal autophagy and implicates reduced insulin signaling in neuroprotective autophagy activation. J. Biol. Chem. 284, 2363–2373.

Yu, W.H., Cuervo, A.M., Kumar, A., Peterhoff, C.M., Schmidt, S.D., Lee, J.H., Mohan, P.S., Mercken, M., Farmery, M.R., Tjernberg, L.O., Jiang, Y., Duff, K., Uchiyama, Y., Näslund, J., Mathews, P.M., Cataldo, A.M., Nixon, R.A., 2005. Macroautophagy–a novel Beta-amyloid peptide-generating pathway activated in Alzheimer's disease. J. Cell Biol. 171, 87–98.

Yu, W.H., Kumar, A., Peterhoff, C., Shapiro Kulnane, L., Uchiyama, Y., Lamb, B.T., Cuervo, A.M., Nixon, R.A., 2004. Autophagic vacuoles are enriched in amyloid precursor protein-secretase activities: implications for beta-amyloid peptide over-production and localization in Alzheimer's disease. Int. J. Biochem. Cell Biol. 36, 2531–2540.

Zeng, X., Overmeyer, J.H., Maltese, W.A., 2006. Functional specificity of the mammalian Beclin-Vps34 PI 3-kinase complex in macroautophagy versus endocytosis and lysosomal enzyme trafficking. J. Cell Sci. 119, 259–270.

Zhang, Y.B., Li, S.X., Chen, X.P., Yang, L., Zhang, Y.G., Liu, R., Tao, L.Y., 2008. Autophagy is activated and might protect neurons from degeneration after traumatic brain injury. Neurosci. Bull. 24, 143–149.